Quaternary International 322-323 (2014) 107–128

Contents lists available at ScienceDirect

Quaternary International

journal homepage: www.elsevier.com/locate/quaint

# New archaeological and geological research at SHK main site (Bed II, Olduvai Gorge, Tanzania)

Fernando Diez-Martín [a,*], Policarpo Sánchez-Yustos [a], David Uribelarrea [b], Manuel Domínguez-Rodrigo [c], Cristina Fraile-Márquez [a], Rosa-Ana Obregón [d], Isabel Díaz-Muñoz [a], Audax Mabulla [e], Enrique Baquedano [f], Alfredo Pérez-González [d], Henry T. Bunn [g]

[a] Department of Prehistory and Archaeology, University of Valladolid, Pza. del Campus s/n, Valladolid 47011, Spain
[b] Department of Geodynamics, Complutense University, Madrid, Spain
[c] Department of Prehistory, Complutense University, Madrid, Spain
[d] CENIEH – Centro Nacional de Investigación sobre la Evolución Humana, Burgos, Spain
[e] Archaeology Unit, University of Dar-es-Salaam, Dar-es-Salaam, Tanzania
[f] Museo Arqueológico Regional, Alcalá de Henares, Madrid, Spain
[g] Department of Anthropology, University of Wisconsin, Madison, USA

ARTICLE INFO

*Article history:*
Available online 7 December 2013

ABSTRACT

This work presents the new round of archaeological research undertaken in SHK Main site since 2009. Through new geological correlations and dating within the Bed II sequence and a new stratigraphic description of the site, new chronological and contextual information is provided for this site. Archaeostratigraphic analysis of the vertical distribution of the archaeological aggregate, a GIS-based restitution of the horizontal associations, and a taphonomic interpretation of the formation processes allow a first intra-site analysis of this high-density anthropogenic patch within the paleo-landscape of the Olduvai basin.



## 1. Introduction

The SHK (Sam Howard Korongo) site is located in the mouth of a lateral gully that debouches in the right bank of the Side Gorge, 1 km from BK and about 2 km from the confluence with the Main Gorge (Leakey, 1971). The site was discovered by S. Howard in the framework of the 1935 expedition to Olduvai Gorge (Leakey, 1974). Surface surveying allowed the identification of a rich accumulation of lithic artifacts and fossil bones in this area. The first archaeological excavations in the site took place in 1953 and 1955, although extensive digs were only undertaken in 1957 (Leakey, 1971). Two different localities were identified in SHK: the Main site was located on the west bank of the gully, at the point where it is opened to the Side Gorge; and the Annex, about 90 m further up the Main site. The combined stratigraphic sequence, from bottom to top, was originally described by Leakey as follows (1971: 165): a) a thick brown clay level exposed both in the Main site and the Annex; b) a 0.75–0.9 m thick and 1.5–0.8 m wide conglomerate filling a channel in the Main site; c) 0.75 m tuff in the Annex laterally related to 2.4 m of tuffs and clayed tuffs overlying the channel in the Main site. The tuff overlying the Annex was originally identified as Tuff IID, although mineralogical analyses carried out later dismissed this correlation and considered that Tuff IID was placed at a higher level in the sequence. The site as described by M. Leakey had, thus, been stratigraphically placed in Middle Bed II, directly below Tuff IIC, although this marker tuff was never identified in the site (Leakey, 1971: Table 1).

The main archaeological horizons were identified in two different sedimentary contexts, on top of the brown clays in the Annex and within the channel conglomerate in the Main site. However, scattered through the clayed tuffs overlying the conglomerate, artifacts and faunal remains were also recovered. The archaeological complex of SHK was interpreted as a pene-contemporaneous occupation representing two complementary environmental situations deposited on top of the underlying clays: an undisturbed by water action hominin occupation on an alluvial plain located in the vicinity of a fluvial channel, where hominin activity also occurred.

* Corresponding author.
*E-mail address:* fernando.diez.martin@uva.es (F. Diez-Martín).

1040-6182/$ – see front matter © 2013 Elsevier Ltd and INQUA. All rights reserved.
http://dx.doi.org/10.1016/j.quaint.2013.11.004

In her publication, Mary Leakey (1971) presents the study of 1064 lithic artifacts (915 tools, plus 26 anvils and 127 light-duty flakes), classified as part of the Developed Oldowan B complex. We should add to these figures a further 3755 specimens included in a generic category of débitage (flakes, cores and waste). Faunal remains were not quantified or described in detail, although a complete *Hippopotamus gorgops* skull, the remains of a herd of *Antidorcas recki* and a tusk of *Elephas recki* were retrieved from the site. Leakey explains that, due to meager financial resources and a small crew of staff working in the field, a considerable amount of archaeological material was discarded and that sieving was not always undertaken (Leakey, 1971: 166). These fieldwork shortcomings explain why the available lithic and faunal collections are biased towards the largest specimens. An undetermined fraction of the débitage and small bone fragments are underrepresented in the collection then curated at the National Museums of Kenya (now in the National Museum of Dar es Salaam). Further analyses of the incomplete fossil collection (Egeland and Domínguez-Rodrigo, 2008) and lithic collection (de la Torre and Mora, 2013) have been subsequently published.

## 2. New archaeological research at SHK main site (2009–2011)

In 2009, in the framework of a survey undertaken by members of TOPP in the Side Gorge, we visited the site. Remains of the channel conglomerate in the Main site and sections of the trench opened in the Annex were still visible. However, the intense erosion produced by a stream flowing down the gully had destroyed most traces of the archaeological work carried out at these sites fifty years earlier. About 40 m to the east of the conglomerate and at the same topographic level, we spotted a significant concentration of *in situ* fossil bones and lithic artifacts eroding from the gully wall, almost at the point in which the gully intersects the Side Gorge. The significance of this archaeological patch plus the technical feasibility of exposing a considerable surface of this large concentration convinced us to open a new trench at this point of the Main site area. Fieldwork here took place in 2009, 2010, and 2011 (Fig. 1). During these three seasons we unearthed a surface of ~40 $m^2$ in the wall of the gully. In the course of this excavation we unearthed two different paleo-landscape features: a) the archaeological patch eroding from the wall in 2009 resulted to be part of a channel filled

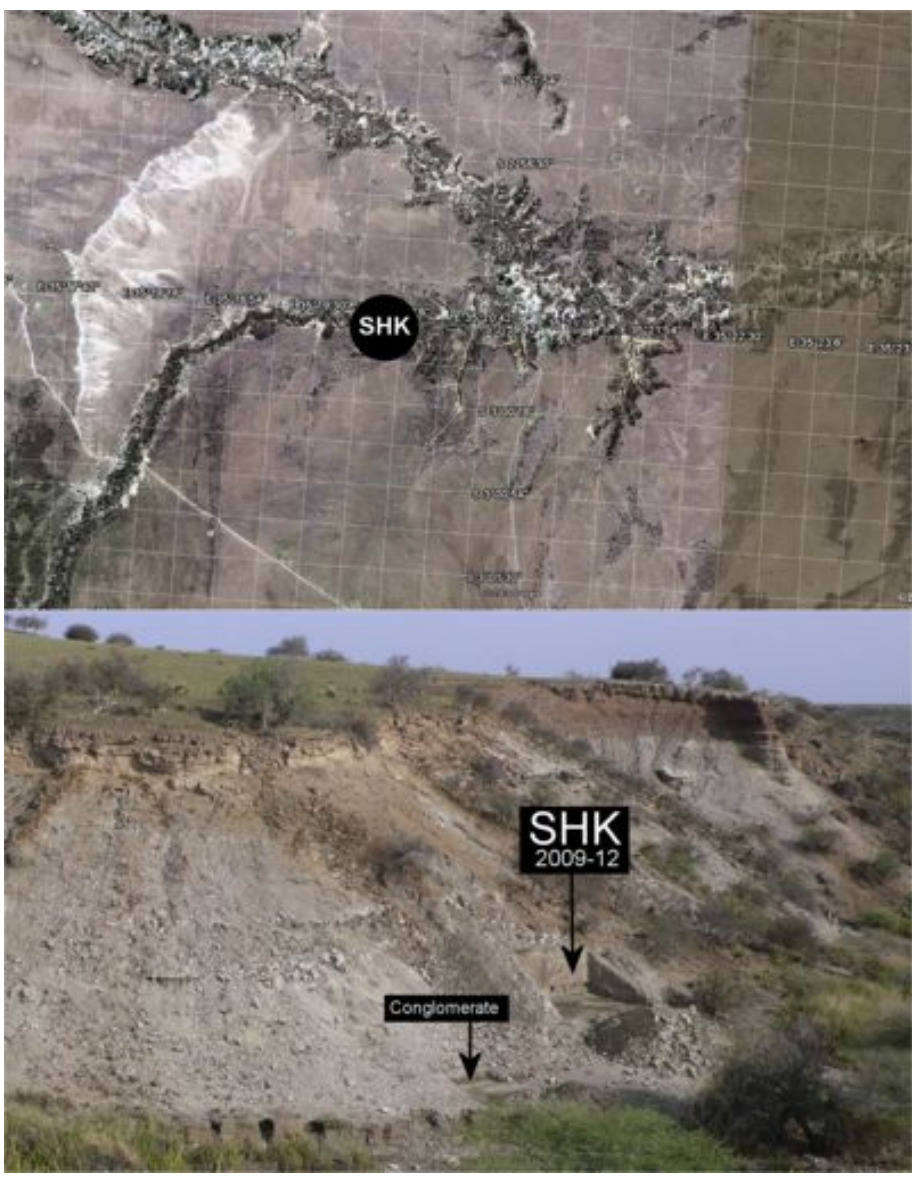


**Fig. 1.** General view of the trench excavated at SHK main site between 2009 and 2011.

with a high accumulation of lithics and fossil bones; b) in the wall and in a higher position, what seemed to represent the bank of the channel also included a significant, although much less dense, accumulation of lithic and faunal remains. An infant *Homo ergaster* skull fragment recovered from this stratigraphic position in 2009 has been recently published (Domínguez-Rodrigo et al., 2012a). A negative topographic feature, formed in the same underlying clays on which all the materials rested irrespective of their topographic position, connected both levels and was interpreted as a paleo-landform related to the channel edge. This work presents the result of our archaeological work at SHK main site, including a geological and stratigraphic description of the locality, a new stratigraphic correlation within the Bed II sequence, the interpretation of the paleo-landscape features recognized, a detailed archaeo-stratigraphic analysis of the different archaeological levels identified, a first taphonomic study of the archaeological materials located within the channel and a preliminary intra-site analysis of the horizontal archaeological associations.

## 3. The geological context

From a geological perspective, SHK (locality 91) is located in Bed II. Here, the archaeological levels excavated by M. Leakey (68a and 68b SHK-west Main site) are bracketed between tuffs IIB and IIC and deposited in sediments corresponding to the Eastern fluvial-lacustrine facies (Leakey, 1971). In the area of SHK the net limit between lacustrine and lake margin sedimentation to fluviatile and aeolian sedimentation can be found (Hay, 1976). The first environment is characterized by broad muddy plains, which are flat, clayish, and with signs of subaerial exposure. Fluviatile and aeolian facies are represented by layers with variable thickness (up to 1 m) of tuffaceous mud massive in aspect. At the contact between both facies, small fluvial channels with coarse bedload and North direction were set up. Archaeological materials were deposited within these channels. SHK is located precisely in one of these channels, located within marker tuffs IIB and IIC.

The stratigraphic sequence (Fig. 2) starts with a 1.2 m thick tuff made of compact and massive tuffaceous siltstone and sandstone. This tuff looks barely reworked, with few non-volcanic contamination, and shows a pale-olive (5Y 6/2) color (according to Munsell Soil Color Charts, 1994; revised edition). Samples of this tuff are currently being analyzed for geochemical and chronological (K/Ar) purposes. On top of this tuff, a 2 m thick clay unit (92% clay, 8% silt, and less than 0.5% sand) mudflat has been developed. It is made of ~2–5 mm sheets with scarce bioturbation (roots and borrows) and abundant nodules and fossilized plant remains (seeds) (Fig. 3). A number of sheets contain a low proportion of tuffaceous silt fining upwards. Color is dark olive brown (2.5Y 3/2) and it shows a homogeneous and cohesive appearance. This unit can be interpreted as a wide mudflat, periodically flooded, where the sedimentation process has been produced by clay decantation. It is slightly tilting (<1%) towards the Main Lake to the North. This facies is similar to the clayey terms of a big floodplain by a meandering river, interpreted as deposits of overbank sheet flow, floodplain ponds, and swamp facies (Nanson and Croke, 1992; Miall, 2006). Hay (1976) underlines the difficulty to characterize with precision this area of the Gorge as lake-margin or floodplain. In the case of the samples observed at SHK, this mudflat shows traits of both fluvial sediments (i.e. deposit geometry, bedding structures and biogenic features) and lake-margin sediments (i.e. texture).

Due either to base level descent or water availability in the alluvial systems, a number of fluvial channels (two on each side of the Gorge) were developed on top of the mudflat. Those located towards the North (left bank) are bigger (around 4–5 m breadth and 1 m depth). Those located on the right bank show 2–2.5 m breadth and 0.8 m depth. Flowing direction is northwards, following the general mudflat tilting. These channels might have been formed when clay was consolidated, considering that banks appear well-defined and no mud plugs, topples in the erosive margin, or slumps in the channel have been identified. Despite moderate mudflat tilting, flux incision in cohesive clay and presence of coarse bedload shows a relatively high-energy formation process for this sedimentary environment. Due to the presence of coarse bedload, these channels have been interpreted as floodplain drainage channels fed up by upstream alluvial systems, which have higher slopes and availability of coarser sediments. They could also be interpreted as crevasse channels, similar to those described in large alluvial rivers (Miall and Smith, 1989). However, large rivers have not been identified in a similar stratigraphic position in the Side Gorge. Once channels are formed, they set off the surface runoff drainage of the mudflat (due to rainfall events or increase of the lake watertable). In these instances, channel flux is occasionally high and it may transport the bedload downstream. From a geo-archaeological perspective, the result of these processes is constituted by a seasonal presence of fresh water in a clayish plain.

SHK main site is composed of 3 archaeological levels (A, B, and C). Two of them (A and B) are precisely located in the filling and the margin of one of these channels, located on the right bank of the Side Gorge (Fig. 4). Due to its proximity to the hillside surface, only one of the channel margins have been preserved (presumably left side considering the channel direction and tilting).

The channel unearthed at SHK has a minimum size of 1.5 m of width and 70 cm depth. At the flat bed there is a 40 cm wide and 20 cm deep scour that defines the channel thalweg. The scour and the first 30 cm of the channel are infilled with a clast-supported conglomerate, carbonate cemented. The matrix is made by sand, silt, clay, and the framework of cobbles, fossil bones, and stone tools. From a lithological perspective, sands are made of quartz, feldspar, and mafic minerals. Most of the pebbles are mafic in origin (basalt, andesite) and, to a lesser extent, granitic and metamorphic (granitic gneiss). Basaltic materials correspond to the volcanic lavas originated in the Lemagrut volcano, while the others come from inselbergs such as Kelogi. General aspect is structureless, with absence of inner structures (bedding, imbrication, clast shortening). Archaeological remains have been found almost exclusively on the upper part of the conglomerate and constitute what has been called the archaeological level A.

The second archaeological level (B) lies on the channel edge, resting directly on the mudflat (Fig. 2). It contains rounded pebbles similar to those found in the channel and mixed with stone tools and bones. The archaeological patch gets denser towards the channel edge. From a geological perspective, both levels A and B could be considered to be penecontemporaneous due to the fact that their distribution is related to the same palaeosurface. Level A was buried first and covered by a 9 cm medium tuffaceous sand layer (57% sand and 42% silt + clay). This is a thin layer, structureless, without archaeological remains and exclusively present within the channel. This level represents a low discharge event which did not overflow the bank. Finally, a 30 cm thick tuff was deposited (presumably corresponding to Tuff 2C) on top of the mudflat and the channel. This level is an ashfall tuff, barely reworked, containing angular crystals of different size in its matrix. However, it is partially cemented and weathered. Textural classification (USDA) suggests a clay loam (39% clay, 29% silt, and 27% sand). Levels A and B coincide with those described by Leakey (1971) as 68b and 68c at the Main site. Hay (1976) describes their respective stratigraphic position as "abundant artefacts and faunal remains filling a channel eroded into claystone and overlain by Tuff IIC" and "scattered artifacts and faunal remains in siliceous earthy reworked tuff and sandstone, probably representing Tuff IIC". These

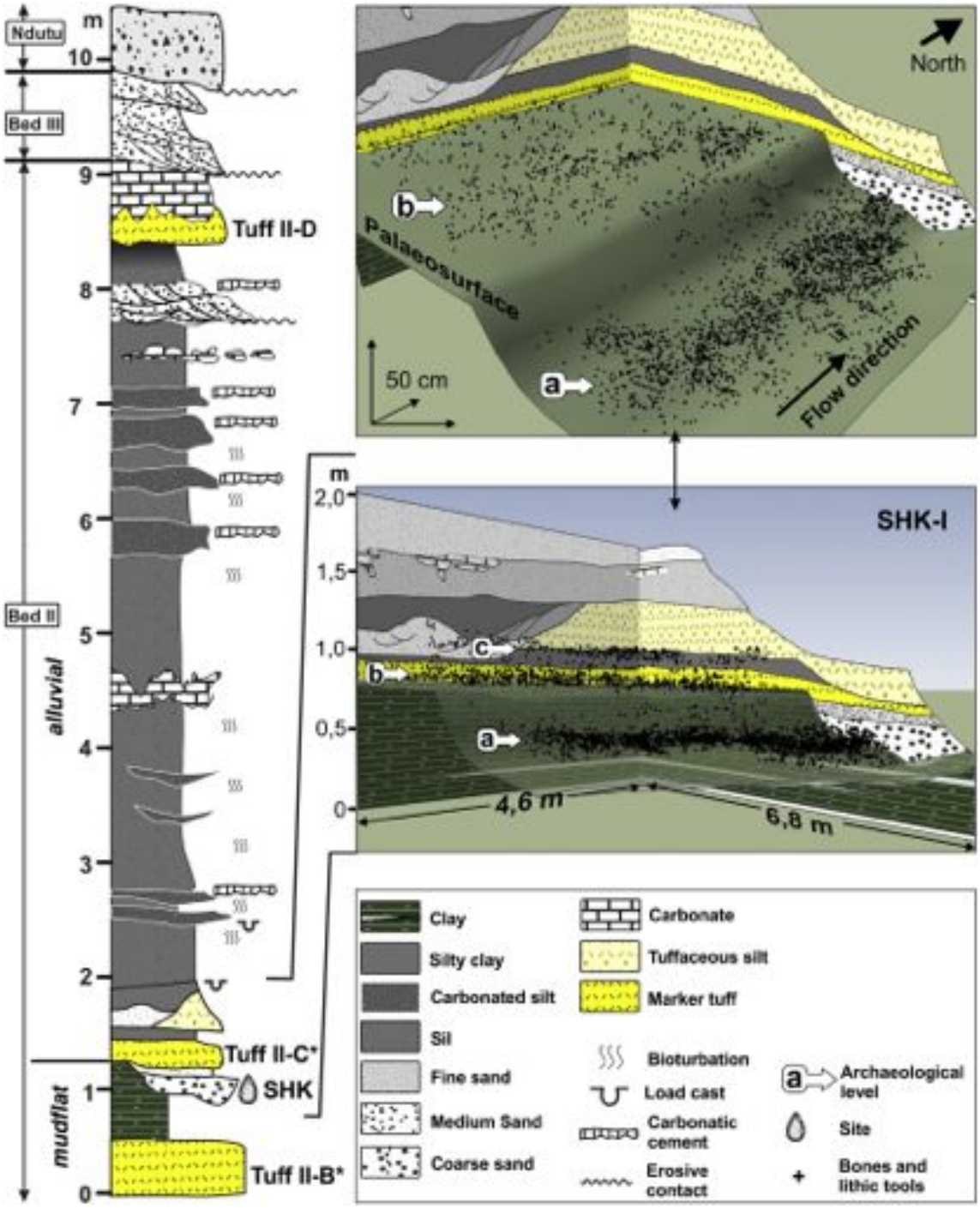


**Fig. 2.** Stratigraphic column of Bed II at SHK (locality 91). Stratigraphic sections and archeological levels a, b and c, projected in 3D. Note the palaeosurface of levels a and b.

authors assume that Tuff IIC covers both levels at the same time, while the medium tuffaceous sand is not distinguished on top of the lowermost level (A).

On top of tuff IIC, a discontinuous clay layer can be identified, showing an irregular and progressive contact with the tuff. It seems to have been subject to edaphic processes, although it is possible that an external clay input has also played a role. Level C rests on top of this layer, which is buried by a tuffaceous silty-clay with carbonate nodules and is pale-yellow (2.5Y 7/3). Facies changes to a substantially more alluvial environment, dominated by thicker and more granulometry sedimentary bodies (i.e. silt). This layer erodes archaeological level C and the top of tuff IIC following the same position than the old channel. The outcrop is too poor to suggest that the channel maintained the same position. Towards the top, the sequence is made of alluvial facies. Tuff IID is located 7 m above level C, almost in the contact with Bed III. A $^{40}Ar/^{39}Ar$ date has been obtained for tuff IID at BK, providing an age of 1.353 ± 0.035 Ma (Domínguez-Rodrigo et al., in press).

## 4. Materials and methods

Fieldwork data were retrieved with the aid of a TOPCON-GPT3105N total station. Spatial features of both archaeological and stratigraphic data were recorded (including nearly 4000


**Fig. 3.** Detail of the clay laminations of the mudflat facies. White dots correspond to small carbonate nodules and plant seeds.

topographic points). This procedure allowed us to create a large high-resolution topographic dataset for the laboratory restitution of data related to: the stratigraphic sequence of the archaeological site, the stratigraphic contextual correlation of the site and its stratigraphy with other stratigraphic features seen in the Bed II outcrops in the area, the 3D reconstruction of the paleo-landsurface unearthed in the course of our excavation (the channel and its overbank), the archaeo-stratigraphic analysis of the archaeological levels, and the intra-site horizontal reconstruction of the different anthropogenic patches. At SHK main site, and during the 2009, 2010, and 2011 field seasons, we opened a total surface of 38.58 $m^2$, with a maximum width in the channel area of 6.98 m and a maximum length into the gully of 6.93 m. The whole archaeological sequences span within a sediment band of 1.254 m Fig. 5 represents the shape of the grid, showing an irregular outline in the southernmost part of the surface (the front in which the basal archaeological horizon deposited within the channel was eroding in 2009). In the course of our excavation, we retrieved a total number of 2833 archaeological specimens (1915 lithic specimens and 918 fossil bones). This amounts to an average density of 73.43 items per $m^2$ (58.56 pieces/$m^3$). Stratigraphic control of our excavation was fairly simple, considering the heterogeneous nature of the deposit, where discrete litho-stratigraphic units can be clearly identified (see the geological section). However, considering the high density of archeological materials unearthed (particularly dense in the case of the channel), our excavation proceeded in 10 cm artificial spits along three different and subsequent strips: a first strip focused on the channel (excavated in 2009 and 2010), a second one in the intersection of the channel and the bank (whose excavation was initiated in 2009 and completed in 2010), and a third one further into the bank towards the wall, excavated in 2011. The recovery of graphic and stratigraphic information in the field was carried out according to the following procedures: fractions of the same strip were horizontally exposed following the spit criterion, photographs of each sector were taken and given a sequential identification, each item was drawn on graph paper at a 1:1 scale reproducing the relative orientation within the grid (orientation for the main length axis of each specimen was taken with the aid of a geological compass while tilting was recorded with the aid of a clinometer, Domínguez-Rodrigo et al., 2012), spatial coordinates for the centroid of each item were given with the total station (Z coordinate was taken on the contact surface where the specimen rested), the correlative code given by the total station to each item was also given to the field drawings and field photographs, and items were removed and identified with their total station code. For the laboratory analysis of the spatial information retrieved in the field we used Autocad and ArcGis 10 software (for the horizontal restitution of data and stratigraphic correlations), and Arch-Plotter and ArcGis 10 software (for the archaeo-stratigraphic analysis).

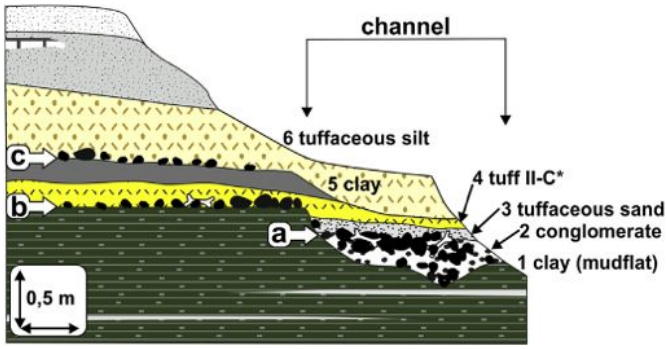


**Fig. 4.** Sketch distribution of the three main archaeological levels (A, B, and C) in the stratigraphic sequence. Levels are numbered from bottom (1) to top (6).

For the vertical analysis of the archaeological occurrences, we have followed an archaeo-stratigraphic method (Canals et al., 2003; Sañudo and Fernández-Peris, 2007; Obregón, 2012). This method aims to approach the stratigraphic analysis of the archaeological data using both longitudinal (North-South) and transverse (East–West) projections of the profiles and sections of the deposit (Canals et al., 2003: 485–486). In this method, each projection represents a bi-dimensional plane that represents a three-dimensional space.

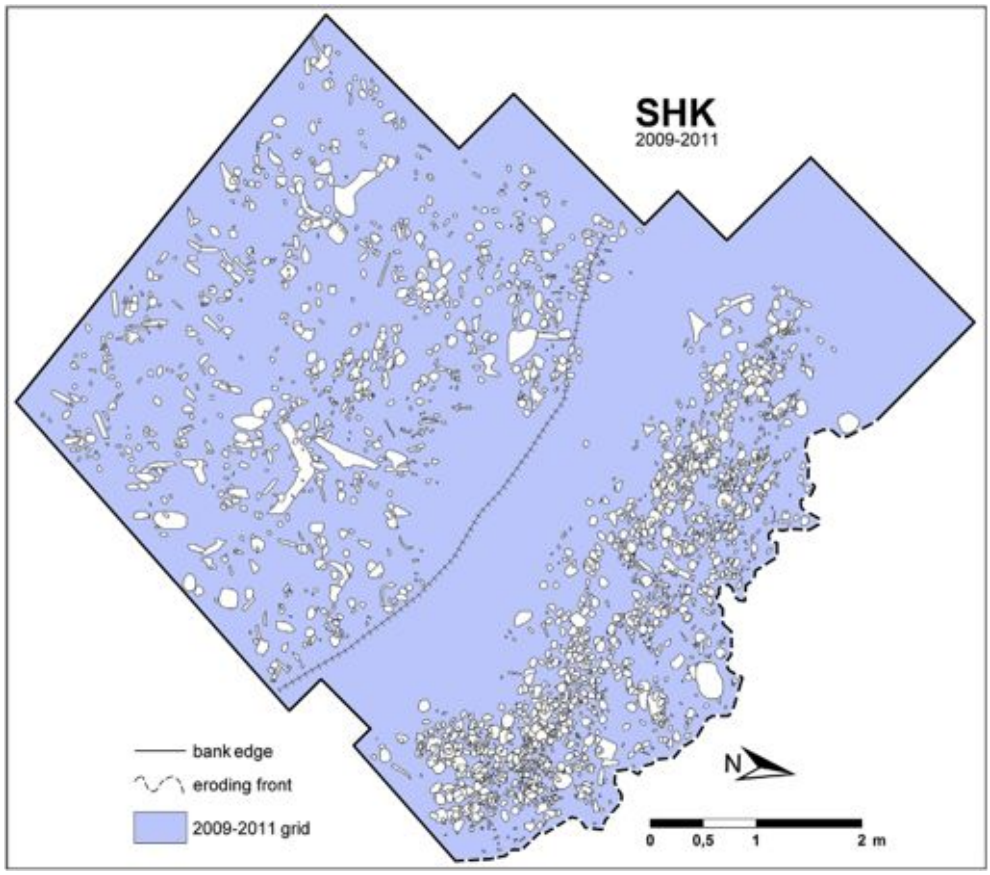


**Fig. 5.** Excavation area opened in SHK between 2009 and 2011.

Main axis for each specimen is the *Z* value, alternatively combined with *X* value (longitudinal profiles) and *Y* value (transverse profiles). Three basic criteria are used for the archaeo-stratigraphic interpretation of vertical projections (Obregón, 2012): a) tilting; b) specimen grouping; c) continuous disruptions or empty surfaces in the vertical sequence. Although this perspective has been very effective in cases of significant homogeneity of the deposits under study, it can also strengthen interpretative consistency in cases like ours, in which archaeological levels correlate with discrete litho-stratigraphic units and paleo-landscape features. High-resolution archaeo-stratigrahic analysis may help to identify different sedimentation rates (including vertical ruptures within homogeneous sediments) and, thus, different high-resolution levels of human occupation within the same deposit, and overcome interpretative problems related to Paleolithic palimpsests (Bailey, 2007; Ferring, 1984; Malinsky-Buller et al., 2011; Vaquero et al., 2012). Using the method and software created for this purpose (Canals et al., 2003; Obregón, 2012), we have proceeded in the following manner: a) creating a net of horizontal and transverse profiles established in intervals of 20 cm depth to identify disruptions, paleo-surfaces, and density variations within the vertical distribution of archaeological items. Combination and intersection of horizontal and transverse profiles constitute a primary routine in the analysis of vertical distributions (Gallotti and Piperno, 2004); b) establishing parameters of control of all the intersections within the archaeological grid through virtual rotations of the grid (control loops – Canals et al., 2003: Fig. 6); c) interpreting synchronicity through the identification of stratigraphic units (based on a number of criteria such as density of archaeological items, presence of discrete features or refitting) referred to as stratigraphic classes (Meignen, 1994) or events (Vaquero et al., 2012).

Regarding the horizontal representation of the spatial associations and the creation of horizontal (2D associations) and vertical maps (for a correct 3D visualization in ArcScene of ArcGis), our laboratory work started out by computerizing our field 1:1 maps (corrected and improved with the concurrence of our field photography). Map vectorization was undertaken with the aid of a digitizing tablet and AutoCad software. Excel files with field coordinates retrieved with the total station were transformed into .dbf files, and exported into a Geodatabase in ArcGis. A shapefile with the representation of Cartesian points was then created and exported into Autocad in order to proceed with the tablet digitizing of the graph maps. Once polygons were created in a Cad file and labeled with their individual code in an associated file, they were exported again into ArcGis in order to join the vector file with the topographic and categorical features of each individual polygon. Each polygon representing an archaeological item was then linked to its *X* and *Y* coordinates (identified with the midpoint of the polygon) and its *Z* value (Gallotti et al. 2011).

## 5. Archaeo-stratigraphy in SHK

The archaeological occurrences span a vertical 1.25 m thickness. Fig. 6 gives the *X*–*Y* vertical projection of the archaeological remains recovered in SHK and clearly shows the existence of three archaeological horizons related to three different stratigraphic units. Level A constitutes a thick accumulation of archaeological materials, particularly conspicuous towards the East of the graphic projection. Maximum thickness of this level reaches 60 cm. Level B appears to be a thinner archaeological horizon, spanning 34 cm of sediment. Finally, Level C represents the least dense horizon, spanning 39 cm. In order to go beyond the use of graphic profiles

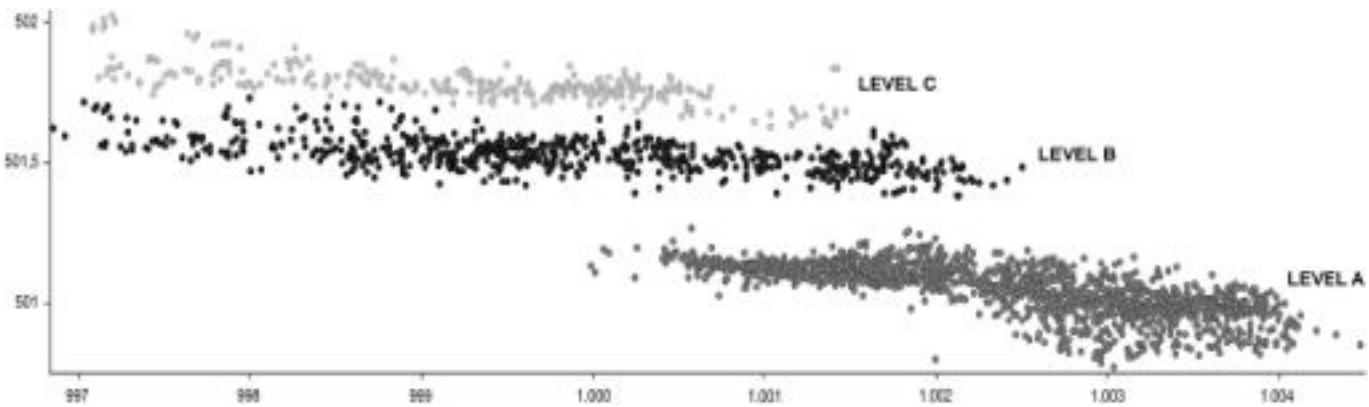


**Fig. 6.** *XZ* vertical projection of the archaeological materials excavated at SHK main site.

with the vertical distribution of items for establishing cursory descriptions of the archaeological occurrences and other related behavioral inferences (Chavaillon et al., 1979; Moncel, 1993; Delagnes et al., 2006), we have applied the archaeo-stratigraphic method of analysis (Canals et al., 2003; Obregón, 2012). For this purpose, we have carried out 75 projections covering the whole surface in spits of 20 cm depth. A total number of 35 spits were established longitudinally (E–W) and a further 40 spits were set transversally (N–S) (Fig. 7). All these projections were analyzed using ArcGis 10 and Arche-Plotter softwares. The combination of longitudinal and transversal sections through the application of control loops and spit intersections allowed us to establish with precision both limits between archaeological horizons and formal disruptions within sedimentation (often imperceptible through visual analyses of vertical distributions).

The most remarkable result of our archaeo-stratigraphic analysis is the subdivision of Level A (the channel) in two different archaeo-stratigraphic units (Fig. 8). This subdivision has been observed in the eastern area of the deposit, where the highest accumulation of archaeological materials occurs. From top to bottom, the first archaeo-unit (A1) includes most of the archaeological patch within the channel (an average density of 80 specimens/m$^2$). It rests on an archaeological gap ~5 cm thick, between 500.0 and 500.95 topographic height. The second archaeo-unit (A2) represents a more scattered distribution of materials (between 15 and 50 specimens/m$^2$) and is identified within an area of 2.5 m$^2$ in the easternmost part of the excavated area. It is significant that the identification of this second archaeo-unit coincides precisely with the area in which the vertical distribution within the channel appears to reach its maximum thickness. If we take this subdivision into account, archeo-unit A1 seems to reproduce a similar depositional pattern (distribution, tilting and thickness) to the one seen in Levels B and C. The depositional anomaly introduced by the archaeo-unit A2 identified at the bottom of the channel claims for a

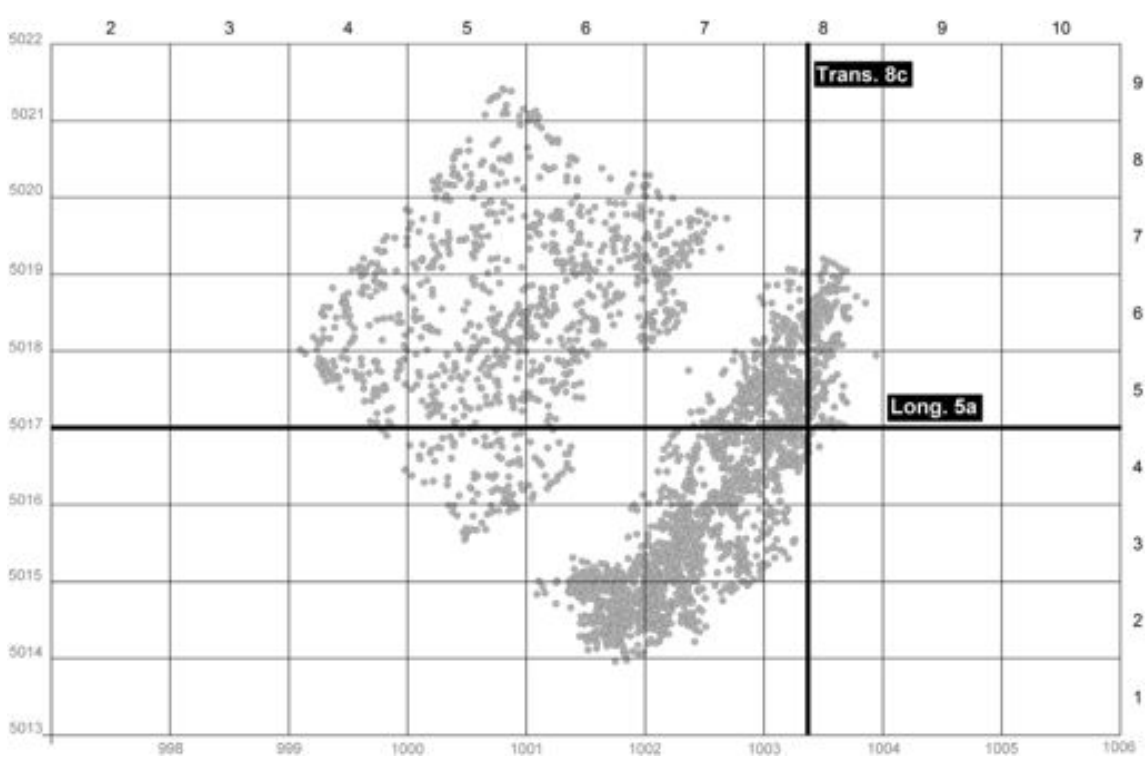


**Fig. 7.** Grid used for archaeo-stratigraphic analysis and example of longitudinal (N–S) and transversal (E–W) projections.

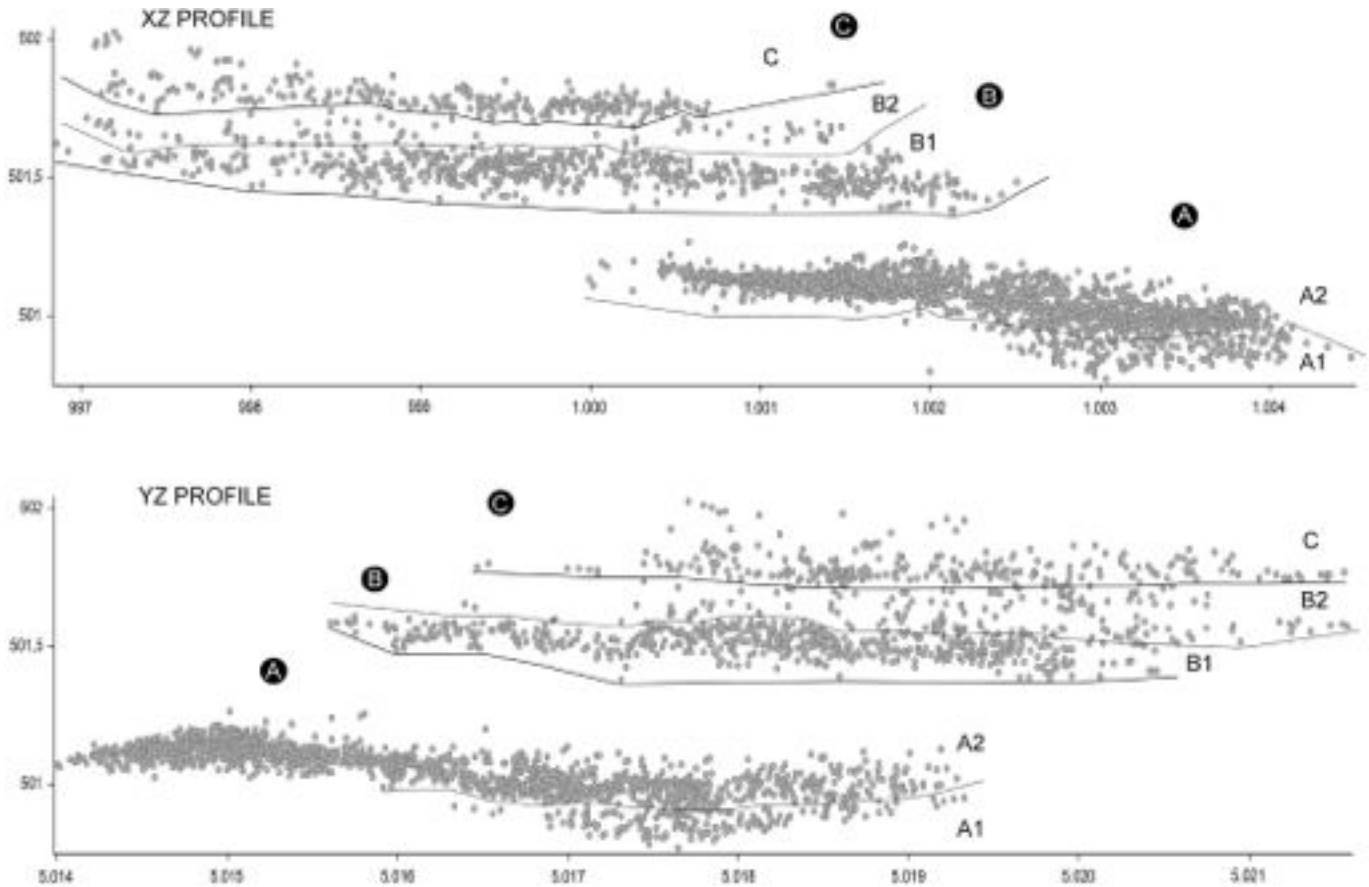


**Fig. 8.** *XZ* and *YZ* projection of the archaeological materials showing the archaeo-unit subdivision of the archaeological levels.

specific depositional history for the archaeological materials included within it. Furthermore, the depositional disruption observed in the archaeo-stratigraphic analysis consistently confirms the existence of two different depositional events within this section of the excavated channel and provides us with a robust analytical tool to conduct further intra-site spatial studies for disentangling spatial associations with behavioral meaning at an event scale. As a cautionary note for the analysis of detailed intra-site associations within the excavated sample, it is important to note that Level B could probably also be divided into two different archaeo-units. This level appears to be a compact, homogenous, and relatively thin layer. This characteristic makes it difficult to establish detailed subdivisions of the deposit (i.e. B1 and B2). However, a number of transversal projections (particularly the one reproduced in Figs. 9.1, 2, and 3) show the existence of stratigraphic gaps that might bear depositional and, probably, behavioral consequences when micro-analysis is applied to the assemblage. Summing up, archaeo-stratigraphic analysis supports the identification of three geological/sedimentary levels (A, B, and C) and five (A1, A2, B1, B2, and C) archaeo-stratigraphic levels within the excavation at SHK main site (Fig. 9.3 and 4).

## 6. Intra-site analysis of the archaeological associations

Fig. 10 shows a plan with the XY distribution of all the remains within the excavated area. According to our archaeo-stratigraphic analysis, we can confidently identify three main archaeological levels, separated by their specific sedimentary context and/or their location in a particular paleo-landscape feature (Fig. 11.1). From top to bottom, Level C was deposited on a clay horizon overlying tuff and was preserved towards the inner part of the grid. A total collection of 151 lithic artifacts and 149 fossil bones were retrieved from this level (52.08 specimens per $m^3$), representing 10.59% of the total sample unearthed in our excavation. The horizontal spatial association of archaeological items included in this level is reproduced in the map in Fig. 11.4. Level B was retrieved on top of the clays underlying the tuff. This level included 355 stone tools and 360 fossil bones (103.03 specimens per $m^3$), 25.24% of the sample (Fig. 11.3). Level A, at the bottom of the sequence, has rendered the largest lithic ($n$ = 1409) and faunal ($n$ = 409) collection (213.13 specimens per $m^3$), accounting for 64.17% of the assemblage. The horizontal distribution of remains retrieved from this level is reproduced in Fig. 11.2. Table 1 shows the distribution of the lithic collection sorted by summary categories and level (Sánchez-Yustos et al., 2014).

**Table 1**
Distribution of lithic specimens sorted by level and general category (following Sánchez-Yustos et al., 2014).

| | Cobbles | Percuss. | Cores | Detached | Large tools (LCTs + choppers) | Total |
|---|---|---|---|---|---|---|
| Level C | 25 | 19 | 30 | 69 | 8 | 151 |
| Level B | 31 | 66 | 66 | 186 | 6 | 355 |
| Level A | 192 | 122 | 188 | 896 | 11 | 1409 |
| Total | 248 | 207 | 284 | 1151 | 25 | 1915 |

Level A constitutes the remainder of a channel eroding the lowermost clay horizon, while Level B represents the channel overbank. Part of the negative landform of the intersection between the channel and the bank was preserved in the excavated

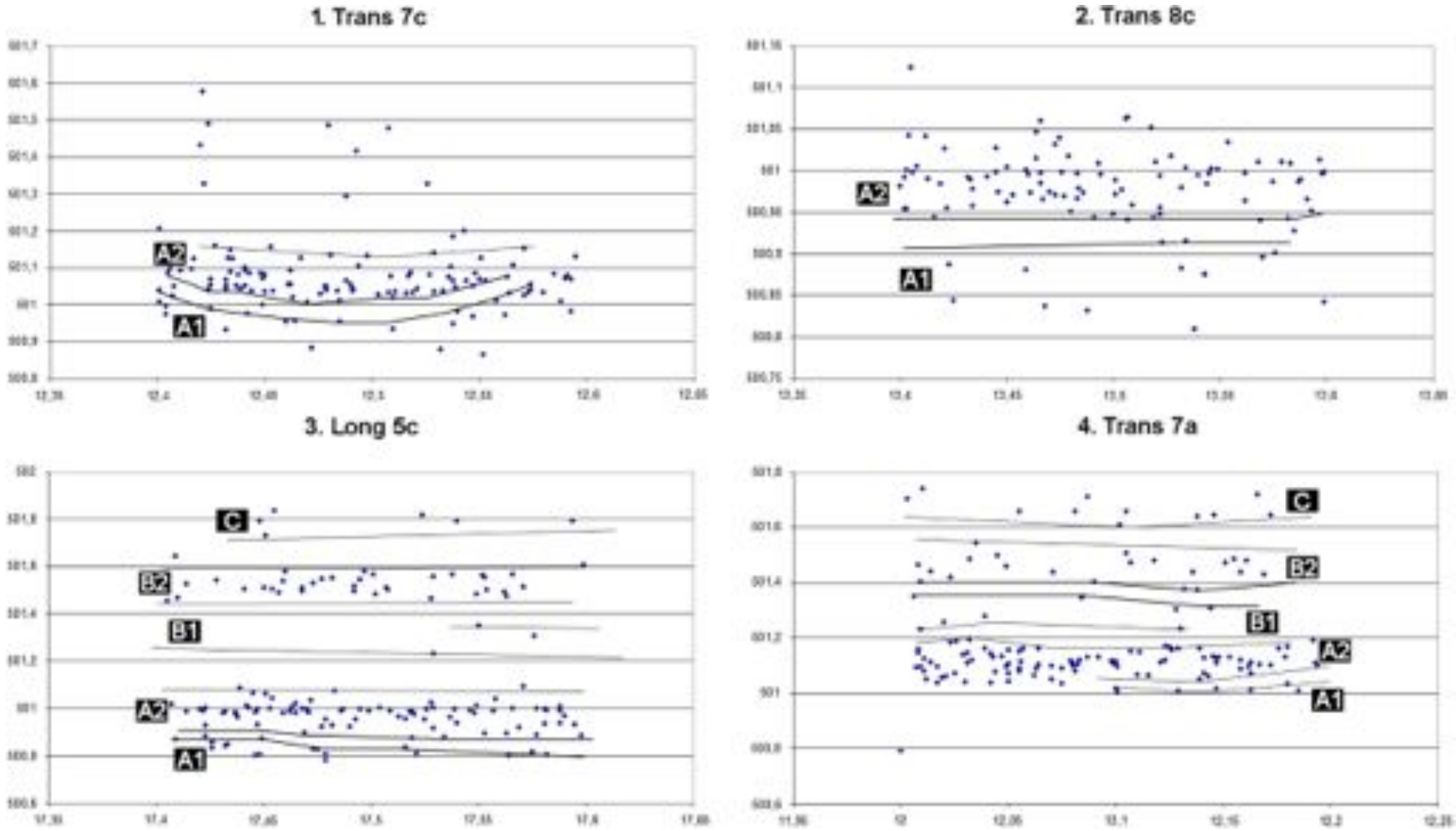


**Fig. 9.** Examples of detailed longitudinal and transversal archaeo-stratigraphic projections, showing depositional gaps between different archaeo-units.

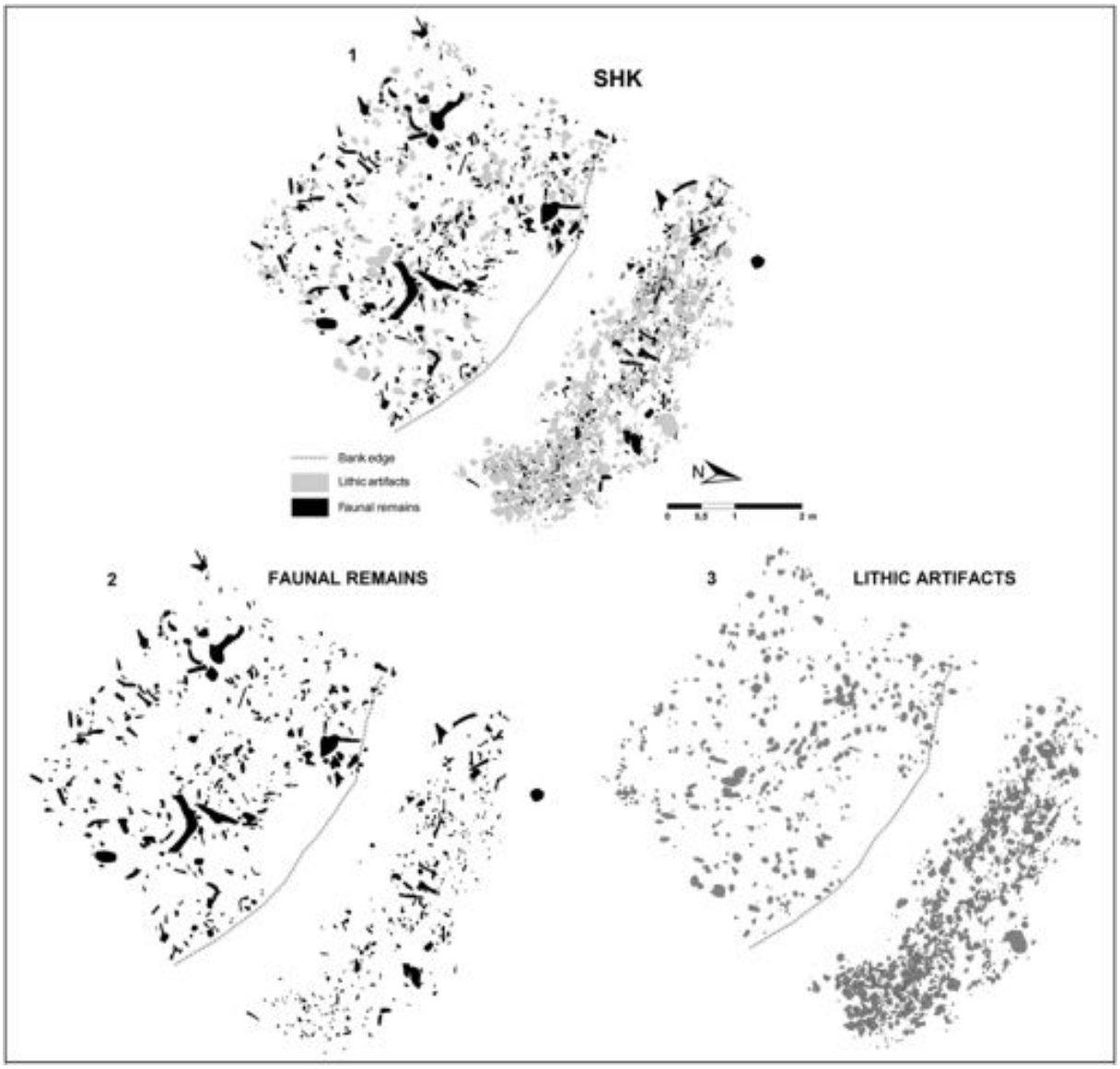


**Fig. 10.** Horizontal association of archaeological remains at SHK: 1. All remains, 2. Fossil bones, 3. Lithics.

area, confirmed by the fact that the same tuff overlying Level B also encapsulated a large fraction of the negative feature. A significant trait observed in our excavation in SHK is represented by the bimodal distribution of the remains (channel/overbank). A prime level of the spatial analysis is, thus, the study of the archaeological associations and their attributes observed within the channel versus the overbank. This issue is of great relevance not only for our diagnosis of SHK as a whole, but for our understanding of the chronological and contextual relationship between these two contextual units: to which extent do these two features represent a homogeneous and well preserved micro paleo-landscape in terms of both time and behavior? To which extent are these features the result of different depositional/erosive events and, thus, represent unrelated behavioral events? In sum, what is the connection between the archaeological materials deposited within these two assemblages? Along with stratigraphic analysis, these questions can be addressed from a perspective that includes the horizontal spatial analysis of the archaeological evidence. For this study we have particularly relied on the lithic samples retrieved from both settings, through the recording of a complete set of attributes on a specimen basis for the SHK lithic collection (Sánchez-Yustos et al., 2014).

### 6.1. *Analysis of taphonomic signals in the channel with respect to the overbank*

A number of attributes can shed light on the taphonomic history of the archaeological materials deposited within the channel environment in SHK (Petraglia and Potts, 1994). These attributes provide insights into the effect of post-depositional disturbances caused by water action in this fluvial context, theoretically more exposed to the effects of disturbance forces (Schick, 1986: Table 5.1), by detecting sample or representativeness biases in the abundant archaeological remains deposited within it. This information can also help to evaluate the existence of any sort of taphonomic heterogeneity in the remains deposited within the channel when compared with the archaeological collection retrieved from the adjacent overbank. Among the attributes selected for this analysis are the study of orientation and tilting of the archaeological materials deposited within the channel (in order to evaluate the effect of high-energy

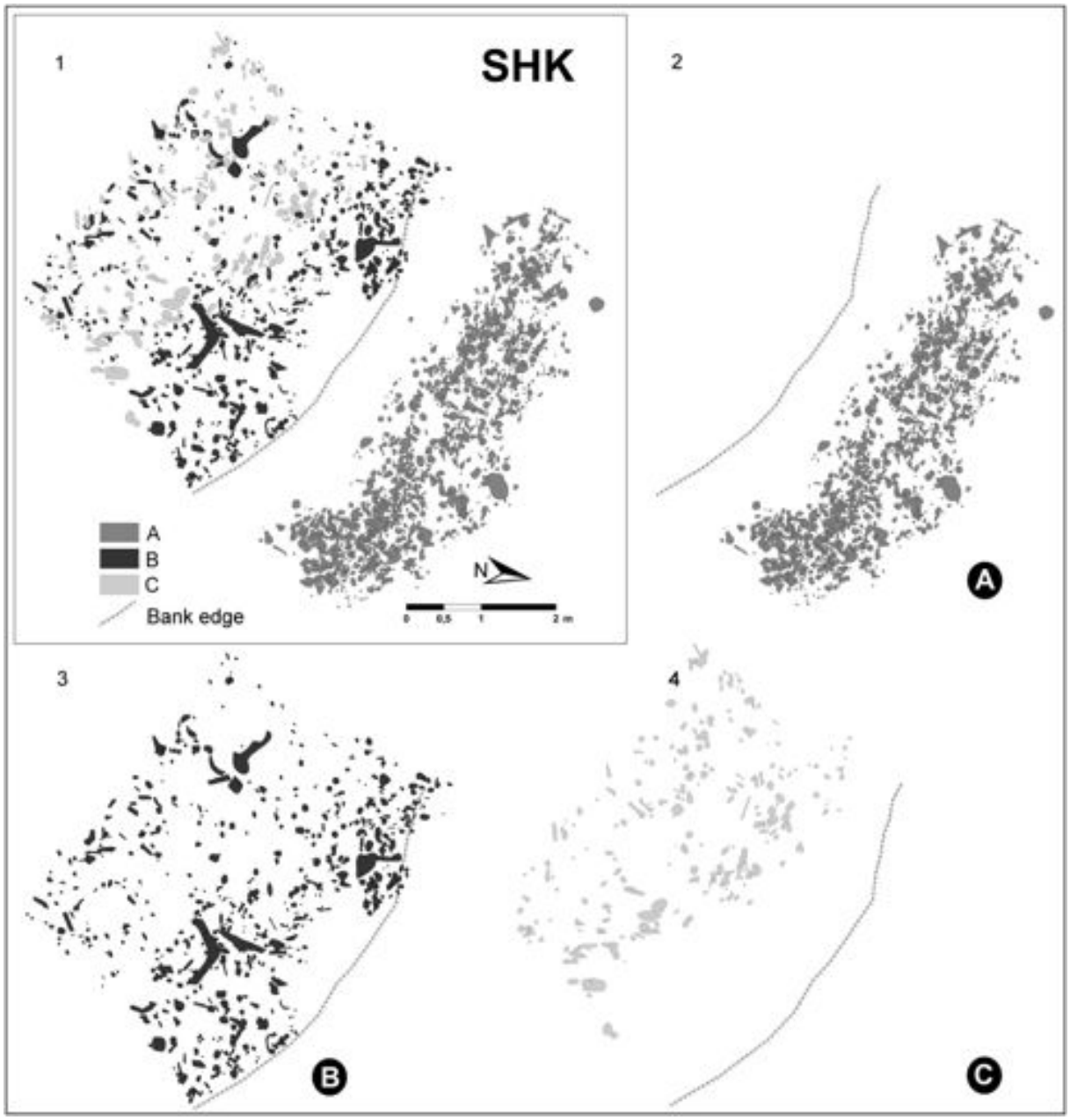


**Fig. 11.** Horizontal association of archaeological remains at SHK sorted by level: 1. All remains; 2. Level A; 3. Level B.; 4. Level C.

disturbance forces in this setting), the effect of polishing and abrasion in the lithic sample, the preservation of the smallest fraction of the knapping process (debris and byproducts ≤25 mm), and the analysis of non-transformed natural cobbles.

Regarding the analysis of water action in the channel, in the course of our excavation we retrieved orientation and tilting data from 336 items (252 lithic specimens and 84 bone specimens) in which a predominant longitudinal axis was prominent and confidently identifiable. Orientation and tilting information was retrieved with a compass and a clinometer following the procedures described by Domínguez-Rodrigo et al. (2012b: 2118). When analyzing the sample as a whole, Woodcock's diagram (Fig. 12.1) suggests a slight tendency to "girdle", but no significant orientation below 95% of the confidence interval can be detected. General uniformity and lack of a specific pattern for the collection can also be seen in the stereogram showing the azimuth orientation of all specimens analyzed (Fig. 12.2) and the general rose diagram (Fig. 12.3) produced for this data. Table 2 shows the results of the statistical analysis undertaken for the analyzed sample, sorted by specimen type. Rayleigh's test shows no unimodal orientation patterns for both bones and stones. However, Watson's test and Kuiper's test show the existence of polymodal orientation (i.e. more than one orientation pattern), particularly conspicuous in the case of the bone sample (Fig. 12.3). Although the data do not completely accord with an intense effect of forces induced by water fluxes in the transportation and redistribution of the archaeological specimens deposited within the channel (Isaac, 1967; Schick, 1986), the pattern differences detected when bones and stones are considered alone are indicative of an active role played by water action in the spatial distribution of bone specimens. Our data supports Schick's observations about the existence of differential behaviors for bones and stones when affected by similar water fluxes (1986, 1987). The influence of water forces within the material deposited in the channel is also confirmed when analyzing

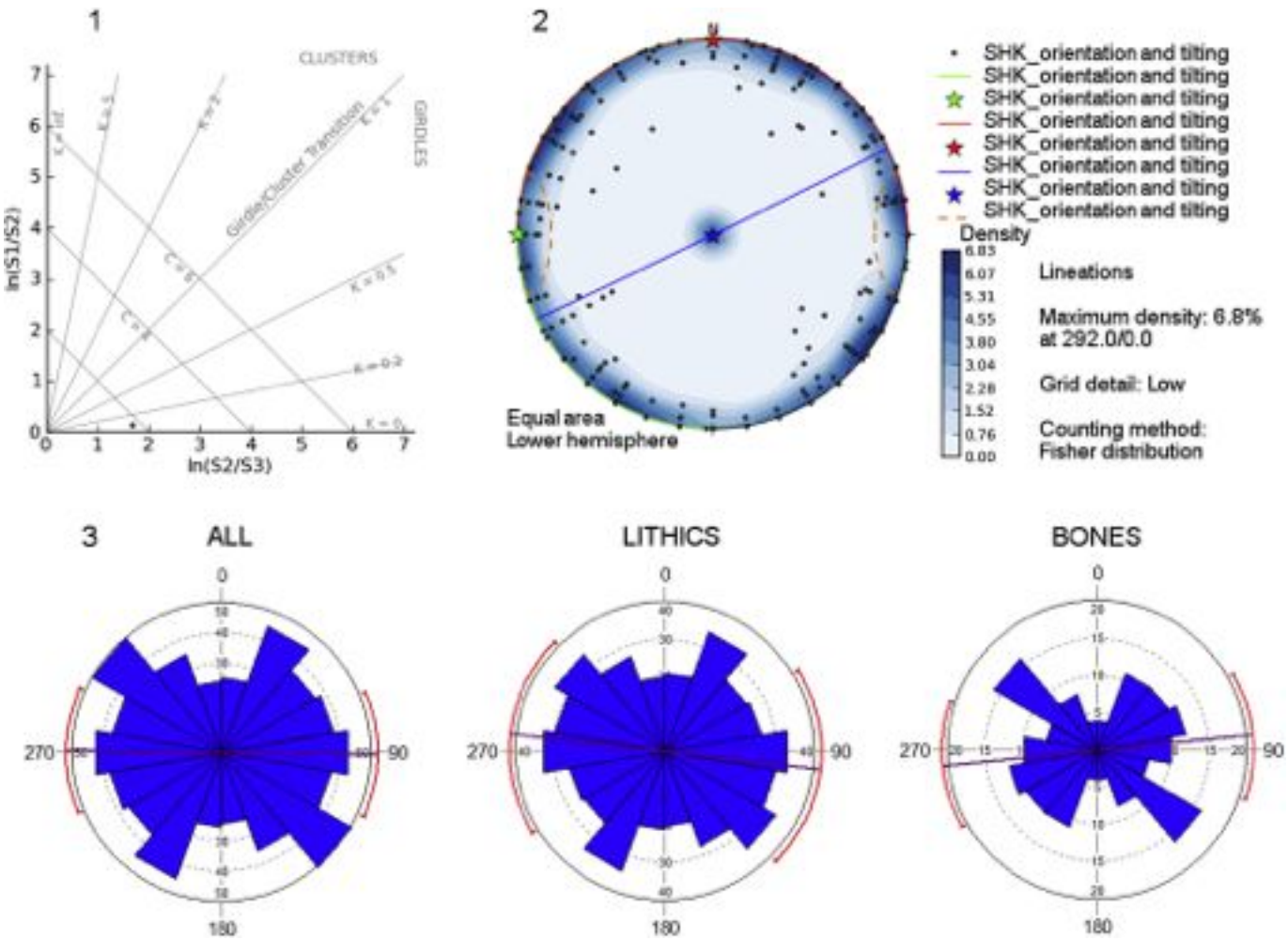


**Fig. 12.** 1. Woodcock's diagram shows a slight tendency to "girdle" (no significant orientation below 95% of the confidence interval); 2. Stereogram showing the azimuth orientation of all specimens; 3. Rose diagrams showing uniform orientation patterns for all items and lithics and a tendency to a bimodal pattern in the case of bones.

the distribution of lithic specimens affected by surface roundness and polishing. For synthetic purposes, we have established two groups attending to artifact polishing: a) specimens in good conditions (mint fresh to fresh), showing sharp edges, ridges and/or no evidence of alteration on their surfaces; b) specimens showing any degree of abrasion (from slight to intense). Fig. 13 shows the spatial distribution of lithic specimens (cores, fragments and detached products) attending to their abrasion category. Significant differences can be observed in comparing the materials deposited in the channel and on the overbank: while 12.48% of the channel collection has been affected by some sort of polishing, only 2.12% of lithics retrieved from the overbank show traces of this kind of alteration. A chi square analysis comparing both collections confirms this point (X-squared = 40.3429, df = 1, $p$-value = 2.131e-10). This observation is in agreement with the analysis of the faunal collection, which showed significant differences in polishing among the materials preserved inside and outside the channel (Domínguez-Rodrigo et al., 2014). However, it is important to remark that the bulk of both lithic collections are constituted by specimens preserved in exceptionally fresh conditions, showing intact edges and ridges. If we take this parameter into consideration (Petraglia and Potts, 1994), it would seem clear that the faunal and lithic materials deposited within the channel have been affected by the effects of water flow in a significantly more intense way than the overbank area. However, it still represents a sample where 87.55% of the lithic specimens have been retrieved in optimal conditions. Although a number of experimental and contextual analyses have pointed out the risk of relying solely on abrasion to evaluate the effect of fluvial forces in the integrity of archaeological assemblages (Harding et al., 1987; Hosfield, 1999; Hosfield et al., 2000), the high percentage of specimens not affected by abrasion in the channel is significantly higher than what is experimentally expected for a collection affected by intense fluvial transport (Shackley, 1974; Harding et al., 1987; Petraglia and Potts, 1994), much higher than collections

**Table 2**
Results of the statistical analysis undertaken for the study of orientation and tilting in the archaeological sample studied: lithics, bones, and whole sample.

| Variable | Lithics | Bones | All |
|---|---|---|---|
| Mean vector (μ) | 96.55 | 84.401 | 90.75 |
| Length of mean vector (r) | 0.066 | 0.181 | 0.092 |
| Concentration | 0.131 | 0.368 | 0.185 |
| Circular variance | 0.467 | 0.41 | 0.454 |
| Circular standard deviation | 66.869 | 52.99 | 62.554 |
| 95% Confidence interval (±) for μ | 58.304 | 60.483 | 67.194 |
| | 134.797 | 108.319 | 114.306 |
| One sample tests | | | |
| Rayleigh test (Z) | 1076 | 2711 | 2.83 |
| Rayleigh test (p) | 0.341 | 0.066 | 0.059 |
| Watson's $U^2$ test (uniform, $U^2$) | 0.142 | 0.205 | 0.265 |
| Watson's $U^2$ test (p) | $0.15 > p > 0.1$ | <0.05 | <0.025 |
| Kuiper's test (uniform, V) | 1754 | 1951 | 2406 |
| Kuiper's test (p) | <0.05 | <0.025 | <0.01 |

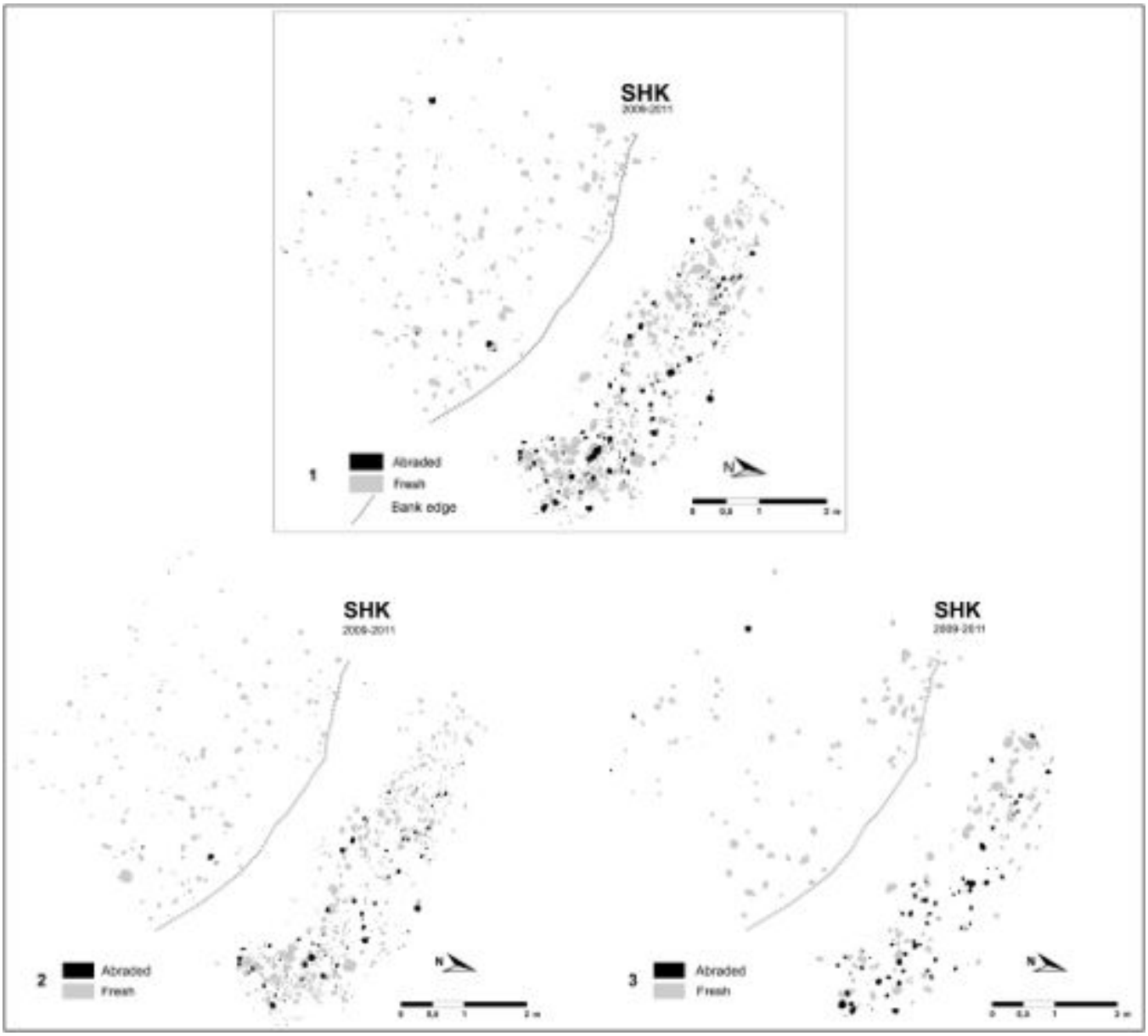


**Fig. 13.** Horizontal association of lithic artifacts (cores, flakes, and retouched specimens) in the channel and the overbank sorted by degree of roundness. 1. The whole collection; 2. Quartz specimens; 3. Basalt specimens.

retrieved from active fluvial contexts (Diez-Martín, 1996), and also higher than the percentage of abrasion described for sites reported to constitute moderately well-preserved sites retrieved from fluvial environments (de la Torre et al., 2008: 248, Fig. 7a).

Experimental studies on fluvial post-depositional processes note that the small fraction of an archaeological deposit constitutes the first part to be washed away by water fluxes. This parameter is particularly useful when studying the integrity of lithic collections (Schick, 1986, 1987; Petraglia and Nash, 1987; Bertran et al., 2012). In SHK, 17.91% of the lithic collection is made up of knapping byproducts (debris, flakes, flake fragments and undetermined fragments) whose maximum length is ≤25 mm. Out of this collection, 54.65% ($n$ = 188) are ≤19 mm. Fig. 14 shows the spatial distribution of lithic specimens ≤25 mm within the channel and on the overbank area. Although this percentage is far from being representative of a primary reduction locus (Schick, 1986; Brown, 2001; Lenoble, 2005), the channel sample includes an estimable proportion of the lithic small fraction (17.45% of the channel collection), which is even a slightly higher percentage than the small specimens retrieved from the overbank (15.22%). Furthermore, when taking into account artifact classes sorted by weight (Petraglia and Potts, 1994: Fig. 1), there are two remarkable differences within the two groups that do not accord with the pattern that should be expected in their respective depositional environments. Fig. 15 shows that the lightest specimens (1–10 g) are significantly more abundant in the channel collection (accounting for 37.85% of the total lithic sample) than in the overbank collection (17.38%). On the other hand, the heaviest specimens (>150 g) contribute to the overbank collection in a significantly higher proportion than they do to the channel assemblage (40.33% versus 15.16%, respectively). Fig. 16 shows the spatial distribution when all artifacts are sorted by size classes. Notwithstanding possible fieldwork bias, the percentage contribution of the small fraction to the total sample retrieved from the channel appears to be higher than what is observed in other Bed II Olduvai sites deposited in moderate to

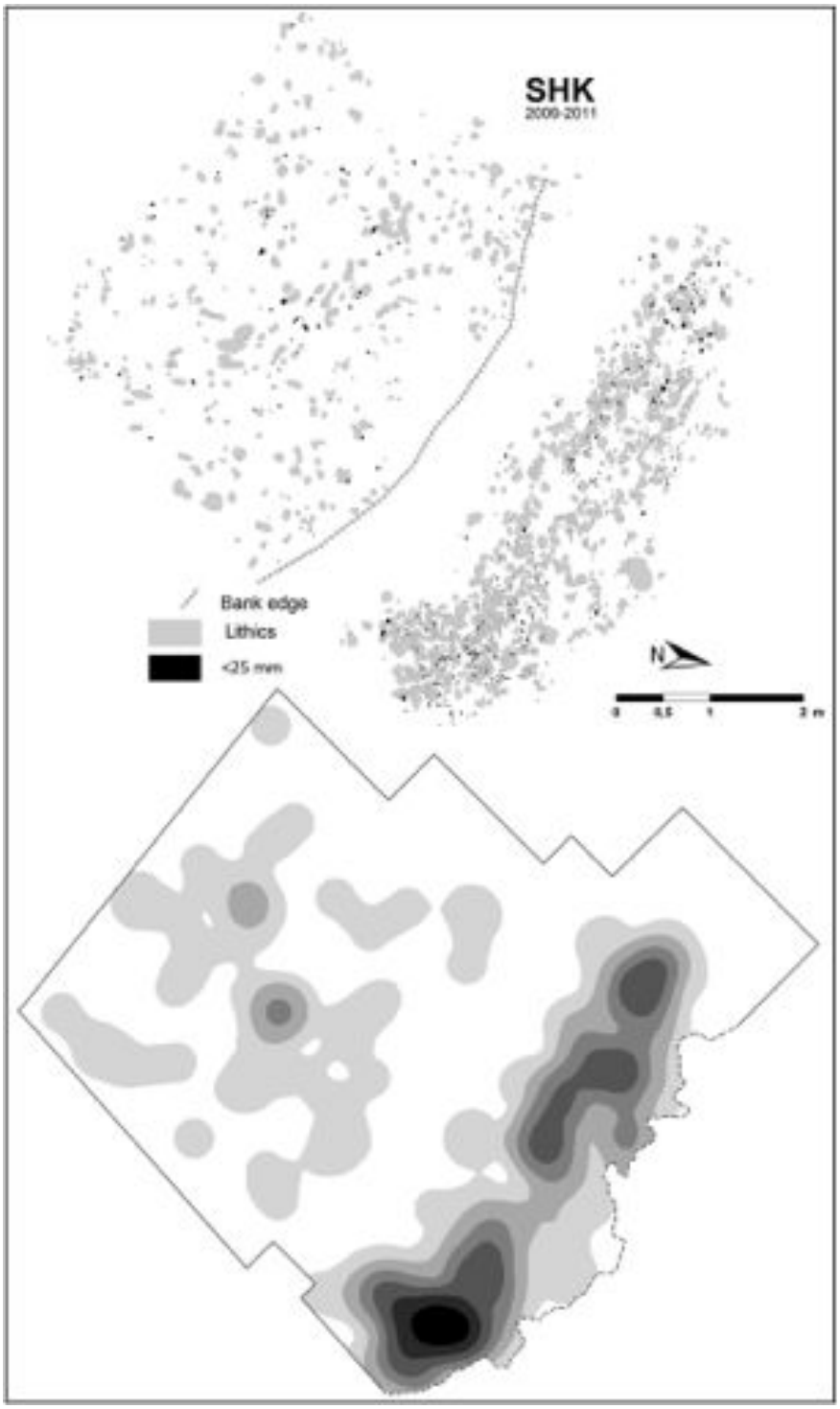


**Fig. 14.** Horizontal association of lithic artifacts ≤25 mm in the channel and the overbank and density map of ≤25 mm specimens.

low energy contexts, such as the case of EF-HR (Leakey, 1971; Torre de la and Mora, 2005: Table 5.1). The dimensional comparison between both <25 mm specimen samples has been analyzed with Rattle, a graphical data mining application for statistical analysis with *R* (Williams, 2009). The boxplot in Fig. 17 shows no significant differences in terms of size and weight when size and weight of the small fraction are compared in the channel and the overbank.

A third trait analyzed in this section is the presence of unmodified pebbles within the channel lithic sample, which could be indicative of the action of natural forces in the configuration of the collection (i.e. a context of transport of cobbles deposited as channel intraclasts in a situation of high-energy water forces). The lithic collection retrieved from the channel in SHK includes a high number of cobbles and nodules, a number of which are significantly large and heavy (including a basalt anvil with a maximum length of

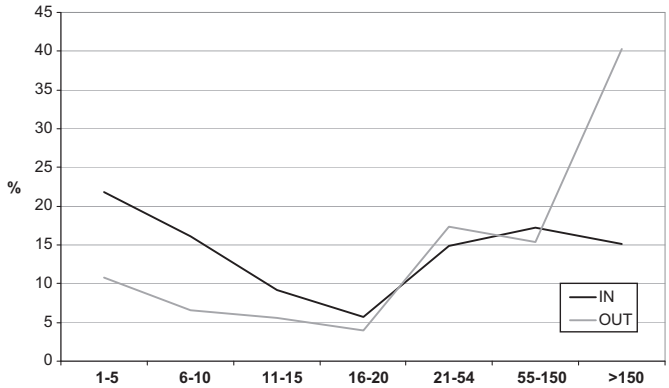


**Fig. 15.** Lithic artifact percentage in the channel and the overbank sorted by weight class (Petraglia and Potts, 1994).

60 cm and 5 kg). Here, modified and unmodified cobbles plus cores represent 39.16% of the total sample. In the channel, in contrast to what it should be expected for coarse alluvial bedload (Goldberg and Macphail, 2006) or in contexts where natural forces might have played a role in random lithic accumulations (de la Torre and Mora, 2005), the assemblage shows a high level of anthropogenic impact. Unmodified cobbles, which could be considered ecofacts in a fluvial coarse bedload, only represent 15% of the collection, while this percentage descends to 9.7% in the overbank area. Furthermore, in the uppermost level (deposited in a low-energy clay context) the percentage of unmodified cobbles rises to 16.9% of the total sample. Fig. 18 shows the spatial distribution of unmodified cobbles within the channel and on the overbank.

### 6.2. Comparison of technological traits in the channel and the overbank

Taking into consideration the important role played in SHK by nodular categories, which account for 39% of the total sample (36.59% in the channel and 46.25% in the overbank area), a first step in comparison aims to analyze the dimensional (length, breadth and thickness) patterns and raw material distribution for unmodified cobbles, percussion elements and cores, in order to detect similarities or discrepancies within these nodular categories in the channel and overbank assemblages and, thus, to evaluate to which extent the abundance of nodular specimens may be either the result of sorting produced by water action (Villa, 1983; Bertran et al., 2012) or an accumulation affected by some degree of hominin-induced patterns. The numerical variables considered here (length, breadth, and thickness) were analyzed using a principal component analysis (PCA). When each of the categories was analyzed separately, a PCA of the unmodified cobbles yielded a two-dimension solution in which the first component accounted for 81.4% of the sample variance and the second component explained 11.2%. This solution offered a comprehensive explanation of the sample, as more than 92% of the sample was properly explained and separated in the Euclidean space (Table 3, Fig. 19.1). The 95% confidence ellipses show that all raw material types overlap and that no significant dimensional differences are detected. This overlap is also documented when comparing the materials inside and outside the channel, although the 95% confidence ellipses tend to show a slightly greater size for the materials outside the channel.

A PCA on the hammerstone sample also explained a large portion of the sample variance (>94%), with a first component explaining as much as 85.4% and a second accounting for 9.3% of the variance (Table 3, Fig. 19.2). There is total overlap in the 95% confidence ellipses when comparing raw material types, although a clear selection is observed when compared with the unmodified cobbles existing inside and outside the channel, since only two materials (quartz and basalt) were used as hammerstones. In comparing the location of hammerstones, those found inside the channel show a tendency to be slightly smaller than those identified outside the channel, as indicated by the confidence ellipses, although the ranges of both samples overlap completely. A PCA carried out on the core sample also produced a two-dimension solution explaining >95% of the sample variance (component 1 = 88.7%; component 2 = 7.6%) (Fig. 19.3). Quartz and phonolite cores are significantly smaller than basalt cores as indicated by the 95% confidence ellipses. There is an overlap in core sizes documented inside and outside the channel, although the latter show a tendency to be slightly bigger.

When considering the complete analytical set (unmodified cobbles, hammerstones and cores), a PCA shows a two-dimension solution accounting for >95% of sample variance (Fig. 19.4), in which a strong overlap is observed, but the 95% confidence ellipses show that cores are significantly smaller than natural cobbles and hammerstones. When comparing the distribution of the nodular types inside and outside the channel, no significant differences were detected, although the trend towards a slightly bigger size outside the channel could be observed.

The four PCA display a series of commonalities, which include the loading of the variables determining each factor. In the four cases, the highest loading variable for the first component is artifact breadth, followed by length and thickness (Table 3). Thickness was the highest loading variable for the second component. The scores are very close because a strong correlation was documented among the dimensional variables used. In all of them, the spatial solution showed that bigger artifacts occurred increasingly with the first factor.

This analysis leads to a number of relevant conclusions. As should be expected in a situation of high anthropogenic impact where a function flux of raw material selection and use is implied, unmodified cobbles and hammerstone size overlap. This means that hominins were taking advantage of natural stones accumulated on the spot (presumably by natural action) to carry out significant percussion activities (in the channel, 32% of cobbles show traces of hammering). However, and contrary to what it should be expected for a conspicuous natural accumulation, cobbles (both hammerstones and unmodified specimens) tend to be slightly smaller in the channel than on the overbank (where hammering is observed in 62.5% of all cobbles). The same pattern is documented

**Table 3**
Correlation values of the variables for each factor according to nodular rock type (natural cobbles, hammerstones and cores). All correlations show $p$ values < 0.05.

| | Cobble | | Hammers. | | Core | | All | |
|---|---|---|---|---|---|---|---|---|
| | Component 1 | Component 2 | Component 1 | Component 2 | Component 1 | Component 2 | Component 1 | Component 2 |
| Length | 0.90 | −0.34 | 0.92 | −0.31 | 0.93 | −0.32 | 0.92 | −0.34 |
| Breadth | 0.92 | – | 0.94 | – | 0.96 | – | 0.95 | – |
| Thickness | 0.88 | 0.45 | 0.90 | 0.41 | 0.92 | 0.35 | 0.91 | 0.39 |

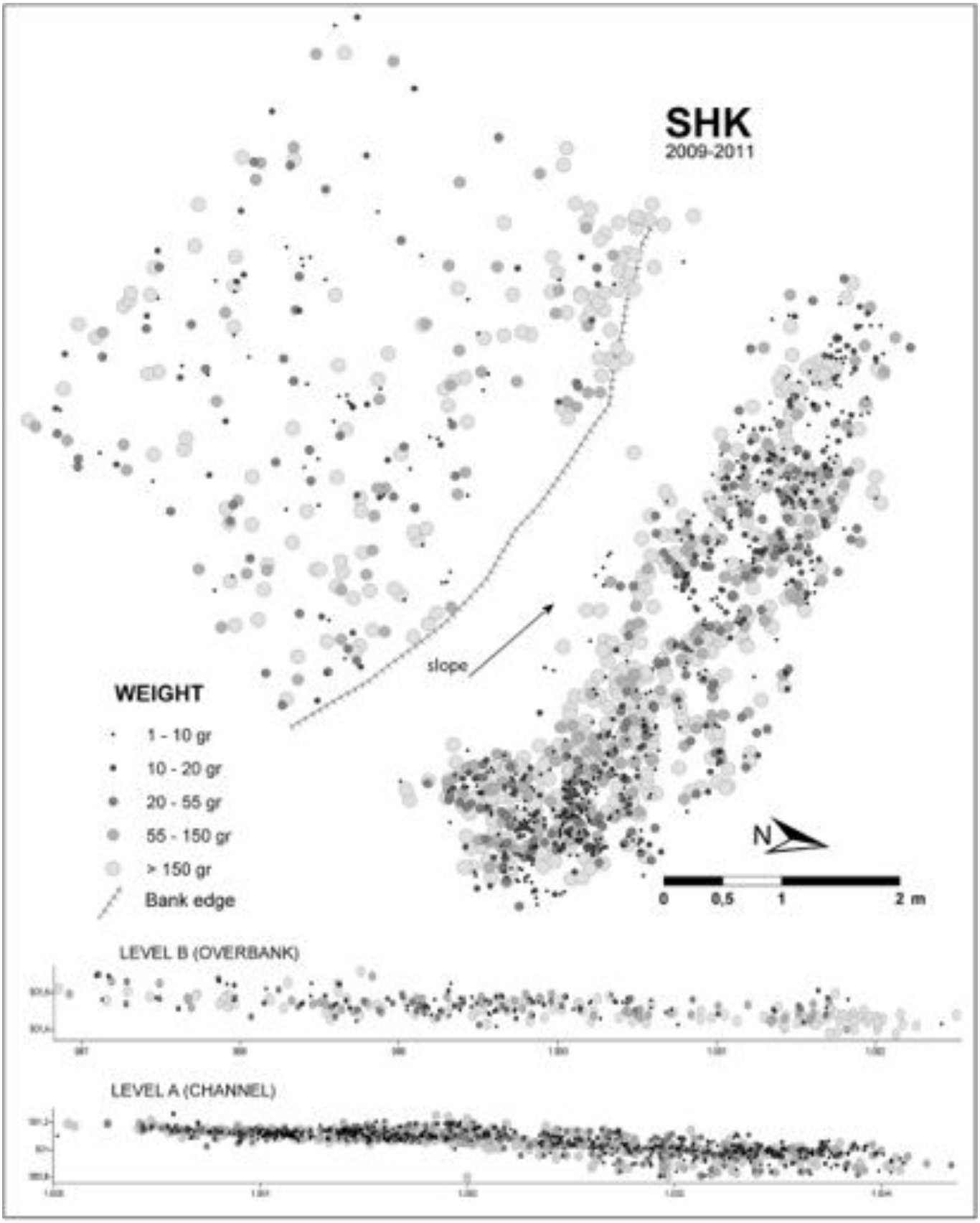


**Fig. 16.** Distribution map of artifact weight classes in the channel and the overbank.

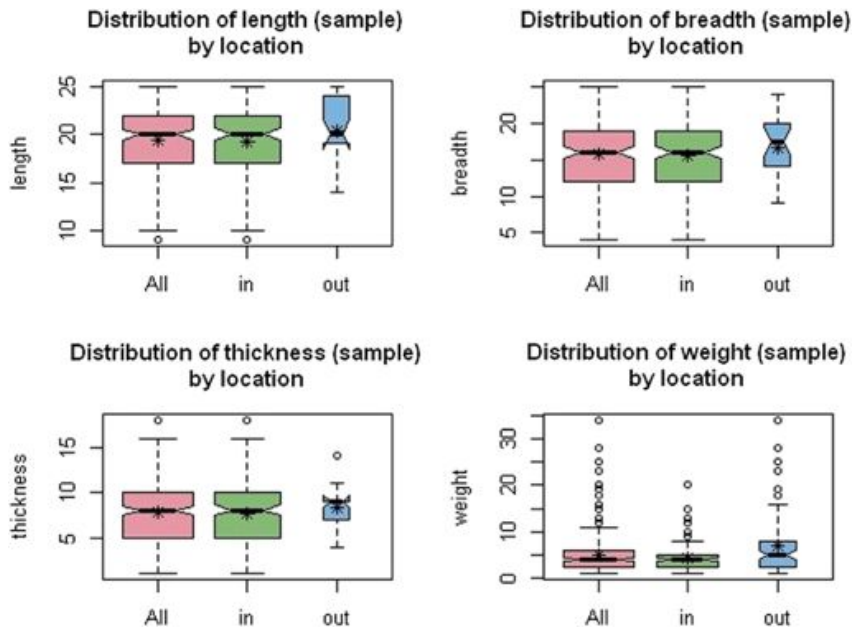


**Fig. 17.** Rattle boxplot showing distribution of ≤25 mm specimens in the channel and the overbank sorted by size (length, breadth and thickness) and weight.

for the core group, indicating that the bias towards the presence of larger nodular morphologies in the overbank might be driven by a behavioral pattern (i.e. selection and transport of specific forms and sizes to undertake a number of percussion tasks).

Despite the fact that core dimensions overlap with the range of cobble dimensions, they tend to be smaller than hammerstones and unmodified cobbles. This pattern is in agreement with the fact that cores, subject to exploitation strategies, have been subjected to

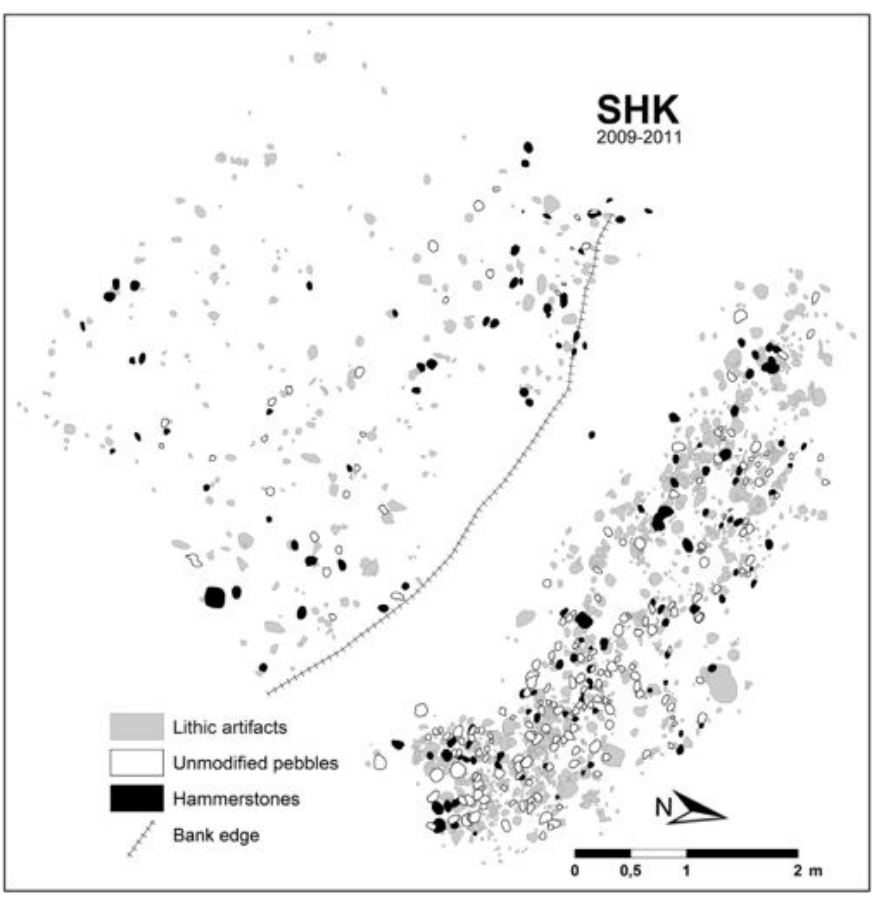


**Fig. 18.** Distribution map of natural cobbles and percussion elements in the channel and the overbank.

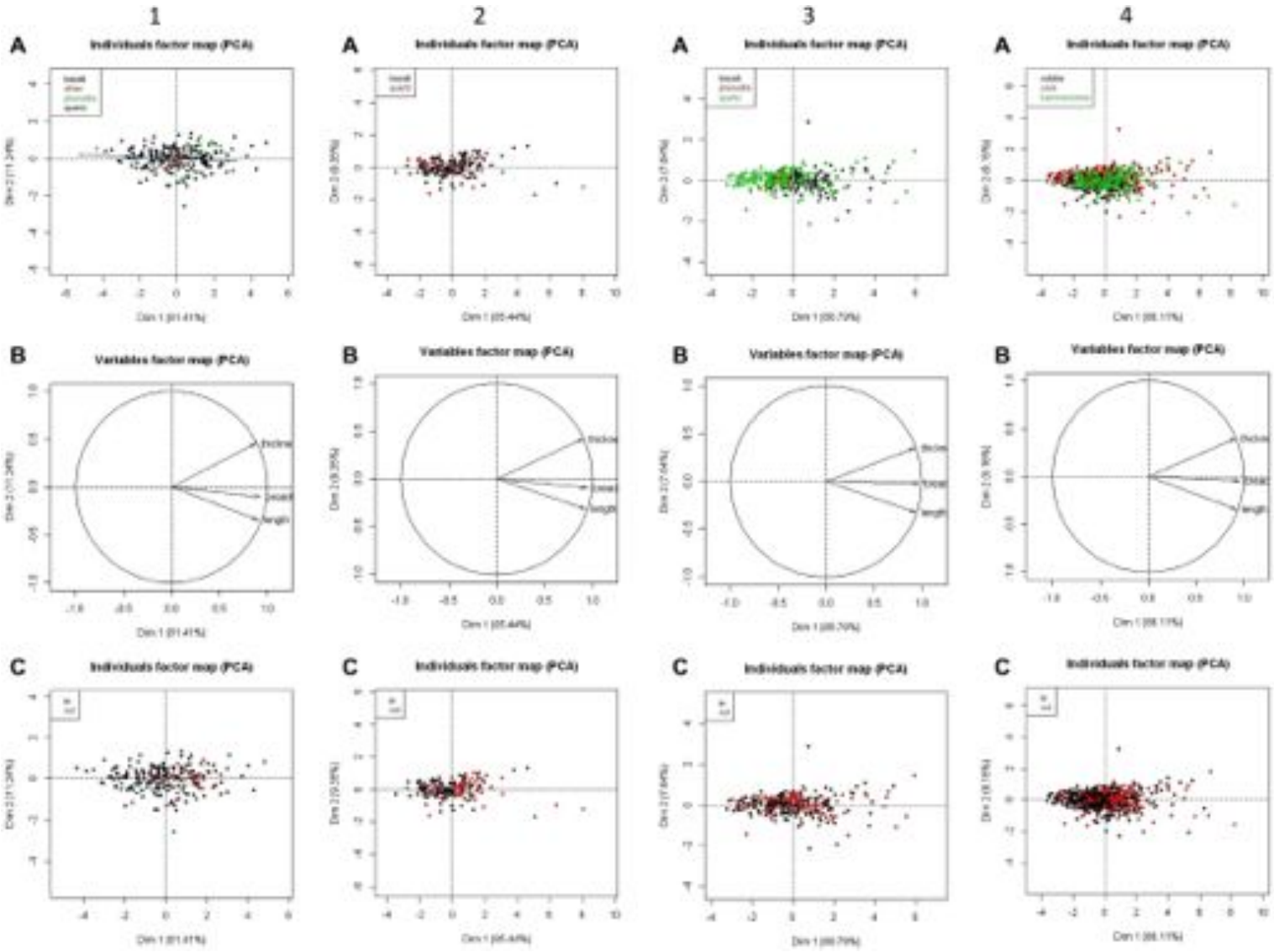


**Fig. 19.** PCA analysis of natural cobbles, percussion elements and cores using numerical variables (length, breadth, and thickness) and categorical variables (location, raw material): 1. Natural cobbles; 2. Percussion elements; 3. Cores; 4. Whole analytical set.

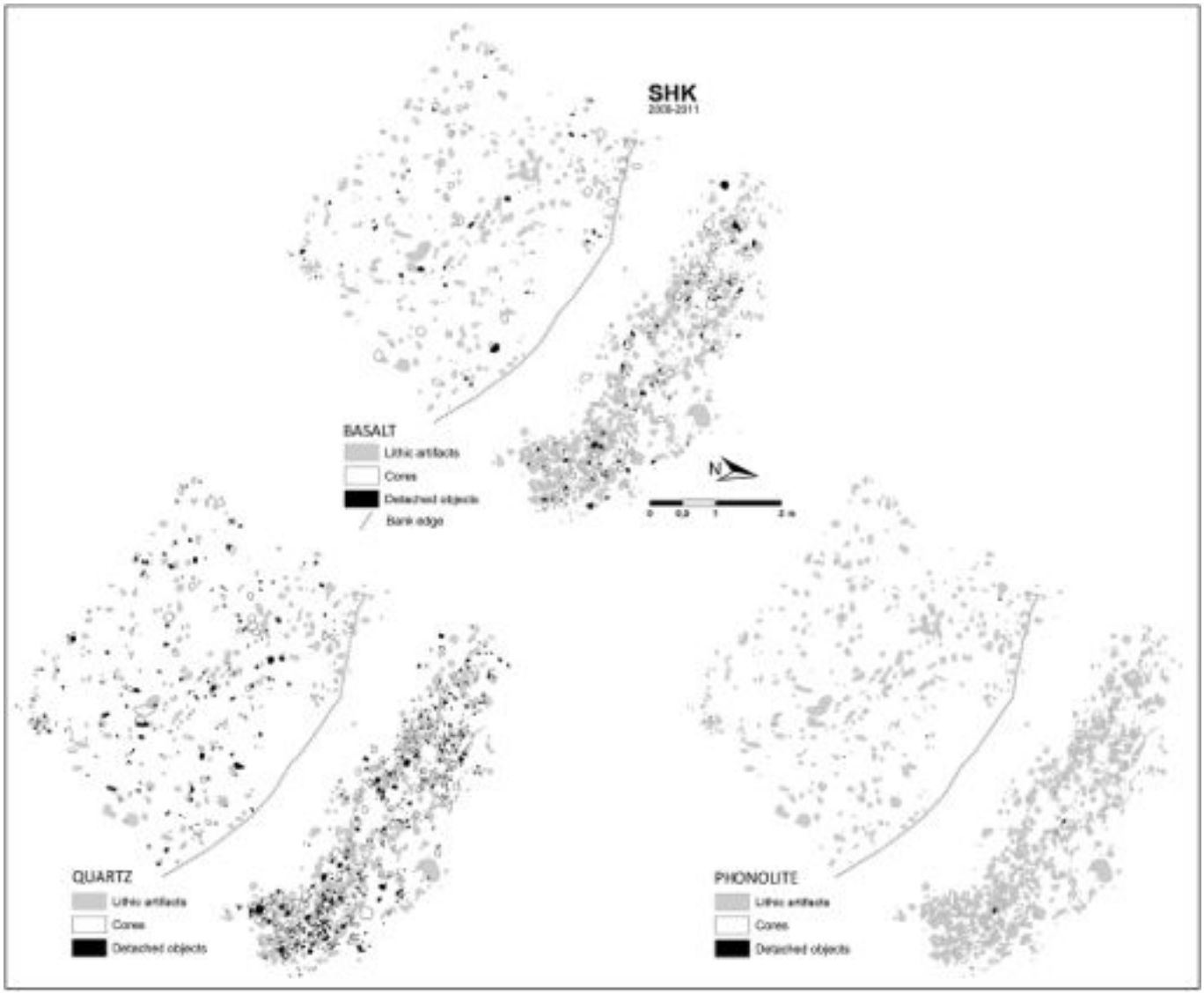


**Fig. 20.** Distribution map of cores and detached products sorted by raw material type: 1. Basalt; 2. Quartz; 3. Phonolite.

mass loss to a variable extent (more intense in phonolite and quartz cores than in basalt cores). As the PCA analysis demonstrates, no dimensional variations can be detected between cores retrieved from the channel and the overbank. Cores constitute a relevant category in both lithic collections, accounting for 14% of the channel assemblage and for 20% in the overbank. Further technical analysis of the distribution of cores in and out of the channel can be undertaken by taking into consideration the different reduction patterns observed within the core category. For this analysis, we have considered the following classification of cores according to the reduction models observed (Sánchez-Yustos et al., 2014): 1. Test cores/unorganized pattern; 2.Unifacial; 3. Bifacial simple (lineal, bipolar); 4. Bifacial orthogonal; 5. Bifacial centripetal; 6. Multifacial/polyhedral; 7. Subspheroidal; 8. Bipolar; 9. Large flake production. Fig. 20 shows the plan distribution of cores and detached objects sorted by raw material type. Regarding reduction strategies, a Chi square analysis reveals the existence of significant differences between the channel and overbank collections (X-squared = 26.419, df = 8, $p$-value = 0.0008902). Fig. 21 reveals that these differences are mostly explained by the fact that most polyhedral and subspheroidal specimens are located within the channel while the overbank assemblage is characterized by bifacial orthogonal reductions and, to a lesser extent, discoid cores. However, both locations show similar rates of unifacial reduction patterns and bipolar cores. Another apparently contradictory trait is that the percentage of test and unorganized cores in the overbank almost double the percentage of these objects in the channel. In a deposit such as the channel excavated in SHK, characterized by a surplus of raw material (large accumulation of unmodified cobbles), a more significant rate of expedient reduction behavior should be expected. Furthermore, in a depositional context intensively affected by hydraulic sorting and redistribution, test specimens and poorly exploited cores should be expected in significantly higher numbers (Bertran et al., 2012).

Regarding detached products, we have first compared the size (length, breadth and thickness) of complete flakes in both locations. The Rattle boxplot in Fig. 22 shows no significant differences in size and weight between flakes. Other categorical traits confirm technological homogeneity between both samples. A chi square analysis of striking platforms (X-squared = 5.6299, df = 5, $p$-value = 0.3439) reveals the preference of plain non-cortical butts, followed at a distance by cortical striking platforms. Other types (in

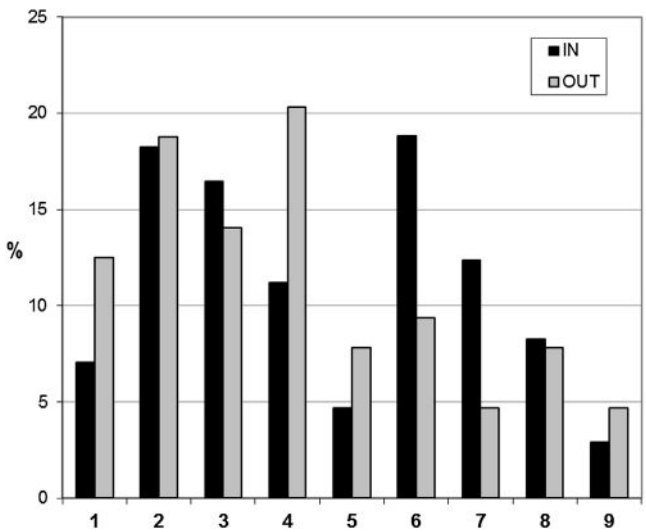


**Fig. 21.** Percentage contribution of core types sorted by location (in or channel/out or overbank) and reduction model (1. Test cores/unorganized pattern; 2.Unifacial; 3. Bifacial simple (lineal, bipolar); 4. Bifacial orthogonal; 5. Bifacial centripetal; 6. Multifacial/polyhedral; 7. Subspheroidal; 8. Bipolar; 9. Large flake production).

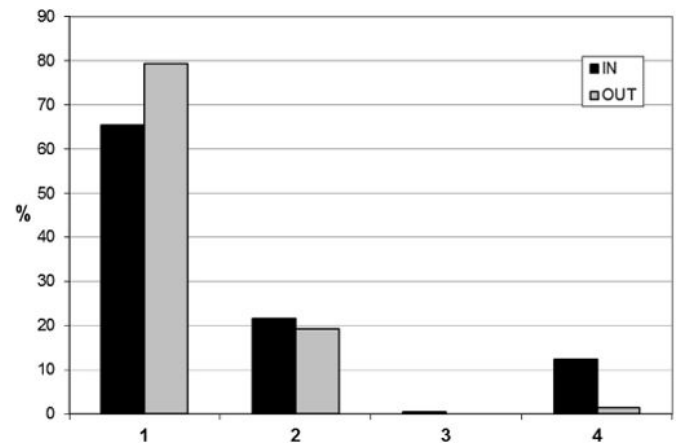


**Fig. 23.** Percentage contribution of plain flakes sorted by location (in or channel/out or overbank) and dorsal pattern (1. Lineal; 2. Orthogonal; 3. Centripetal; 4. Unorganized).

this order, pointed, lineal, bifaceted and multifaceted) are marginal. When the flake sample is classified according to Toth's types (1982), a chi square test shows no differences between both samples (X-squared = 9.5528, df = 5, *p*-value = 0.08895), showing the prevalence of non-cortical type 6 specimens in both the channel and the overbank. The same proportion of other flake types (particularly represented by types 5 and 2) has been observed. However, discrepancies can be observed when flake dorsal patterns are considered (Sánchez Yustos et al., 2014). These differences can be particularly observed in the percentage contribution of non-organized dorsal patterns (significantly more abundant in the channel flake sample) and, to a lesser extent, higher rates of lineal patterns in the overbank (Fig. 23).

Finally, retouched flakes have also been studied for this technical comparison. The Rattle boxplot in Fig. 24 shows that, although retouched implements are slightly larger in the overbank collection, no significant size differences have been detected. When the morpho-types of retouched flakes are considered (Sánchez-Yustos et al., 2014), a chi square analysis shows no differences (X-squared = 10.8443, df = 7, *p*-value = 0.1456). In both cases, denticulates, scrapers, perforators and composite tools (mostly scraper + denticulate associations) have been recognized in similar proportions.

## 7. Conclusions

Research undertaken in SHK main site during our 2009–2011 fieldwork has produced the following data, relevant for a more comprehensive interpretation of this site within the Bed II sequence:

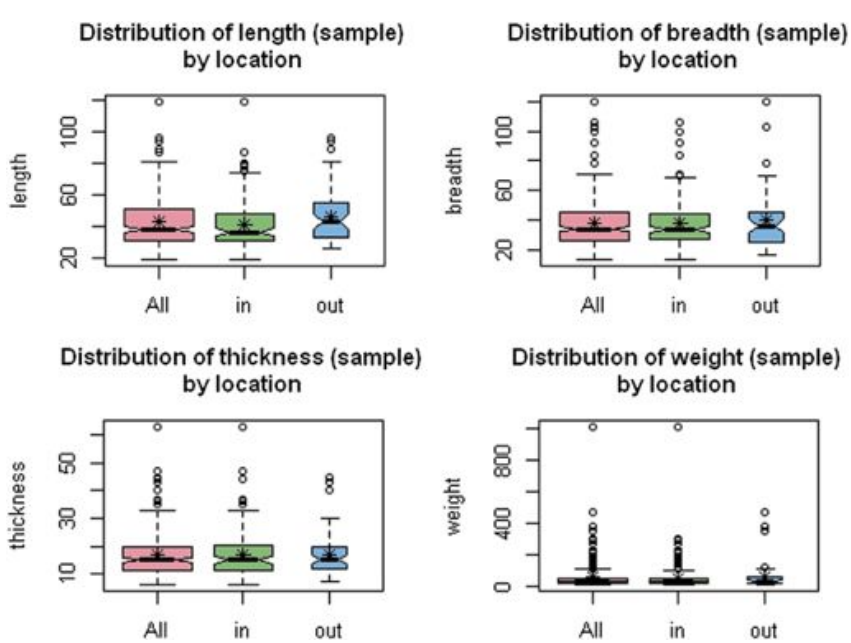


**Fig. 22.** Rattle boxplot showing distribution of complete flakes in the channel and the overbank sorted by size (length, breadth and thickness) and weight.

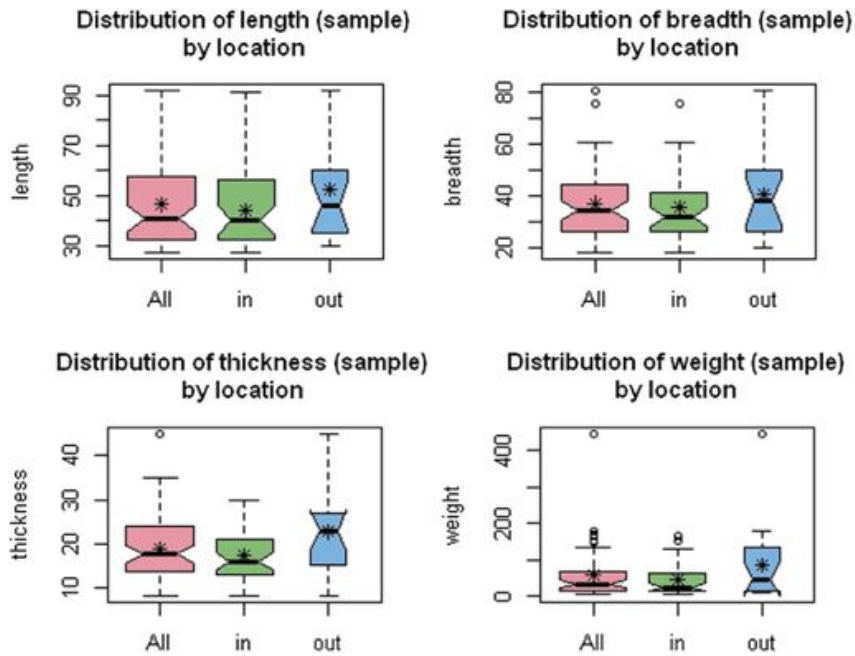


**Fig. 24.** Rattle boxplot showing distribution of retouched flake types in the channel and the overbank sorted by size (length, breadth and thickness) and weight.

- Our excavation has unearthed a well-preserved portion of the local paleo-landscape present at SHK, consisting of a fluvial channel and part of its adjacent overbank, both covered by the same tuff deposit (presumably corresponding to Tuff 2C). Remarkable accumulations of fossil bones and lithic artifacts occurred on both features, considered to be contemporaneous features of the same landscape. A third, more modern, archaeological unit has been deposited on top of tuff 2C within a fine-grained clay matrix.
- The combination of stratigraphic observations and the vertical distribution of the archaeological materials shows the existence of three main litho-stratigraphic levels. From bottom to top: Level A represents the conglomerate within the channel; Level B is constituted by the channel bank; and Level C represents a later event not related to the fluvial environment represented by Levels A and B. The use of an archaeo-stratigraphic approach has allowed us to subdivide Levels A and B in four archaeo-stratigraphic units (A1, A2, B1, and B2). These units have been identified by the presence of archaeological gaps within the sedimentary sequence and indicate different depositional events within the sedimentary continuum. Intra-site spatial analyses will use these archaeo-stratigraphic units in order to identify micro-spatial classes or events with behavioral meaning.
- Regarding intra-site spatial analyses, this paper has focused on investigating the nature of the archaeological relationship between the anthropogenic patches documented in the channel and on its overbank, based on the consideration of a number of parameters with taphonomic and/or technological meaning. As Level C has only been excavated partially and identifies an independent depositional event, it has been excluded from this preliminary spatial study. Orientation and tilting data retrieved from an archaeological sample recovered in the channel show no specific patterns related to fluvial impact in the lithic accumulation. However, the analysis shows that bones have been subject to preferential orientation, suggesting that fluvial forces might have played a role in the accumulation of the anthropogenic patch. Other parameters, such as lithic polishing, percentage contribution of the small lithic fraction, and distribution of unmodified cobbles, reinforce the idea that no significant taphonomic differences can be inferred between both locations.
- The comparison of a number of morpho-metric and technological traits between the lithic collections retrieved in the channel and the overbank (size of natural cobbles, hammerstones and cores, core types, flake size, flake types, and retouched flake types) show no significant metric and technical differences between both collections.
- Summing up, taphonomic, metric and technical data confirm that, despite their different depositional context, Levels A and B show remarkable homogeneity and that they may constitute fractions of the same occupation event. Further micro spatial analyses at an archaeo-unit level may identify signals of behavioral events within the fluvial context identified at SHK main site.

## Acknowledgements

We wish to thank Tanzanian COSTECH and the Antiquities unit for permits to conduct research at Olduvai Gorge. We appreciate major funding provided by the Spanish Ministry of Science and Innovation through the National Plan I + D + I 2010-2012 (reference HAR2010-18952-C02-02).

## References

Bailey, G.N., 2007. Time perspectives, palimpsests and the archaeology of time. Journal of Anthropological Archaeology 26, 198–223.
Bertran, P., Lenoble, A., Todisco, D., Desrosiers, P., Sørensen, M., 2012. Particle size distribution of lithic assemblages and taphonomy of Palaeolithic sites. Journal of Archaeological Science 39, 3148–3166.
Brown, C.T., 2001. The fractal dimensions of lithic reduction. Journal of Archaeological Science 28, 619–631.
Canals, A., Vallverdú, J., Carbonell, E., 2003. New archaeo-stratigraphic data for the TD6 level in relation to Homo antecessor (Lower Pleistocene) at the site of Atapuerca, North-Central Spain. Geoarchaeology 18, 481–504.
Chavaillon, J.C., Hours, N., Piperno, M., 1979. From the Oldowan to the Middle Stone Age at Mela-Kunturé (Ethiopia). Understanding cultural changes. Quaternaria 21, 87–113.

Delagnes, A., Lenoble, A., Harmand, S., Brugal, J.-P., Prat, S., Tiercelin, J.-J., Roche, H., 2006. Interpreting pachyderm single carcass sites in the African Lower and Early Middle Pleistocene record: a multidisciplinary approach to the site of Nadung'a 4 (Kenya). Journal of Anthropological Archaeology 25, 448–465.
Diez-Martín, F., 1996. El Paleolítico inferior en el Valle Medio del Duero. Los yacimientos de Tovilla y Las Cotarras (Tudela de Duero y Traspinedo, Valladolid). Unpublished M. A. dissertation. University of Valladolid, Valladolid.
Domínguez-Rodrigo, M., Pickering, T.R., Diez-Martín, F., Mabulla, A., Musiba, C., Trancho, G., Baquedano, E., Bunn, H.T., Barboni, D., Santonja, M., Uribelarrea, D., Ashley, G.M., Martínez-Ávila, M., Barba, R., Gidna, A., Yravedra, J., Arriaza, C., 2012a. Earliest Porotic Hyperostosis on a 1.5-million-year-old hominin, Olduvai Gorge, Tanzania. PLoS ONE 7 (10), e46414.
Domínguez-Rodrigo, M., Bunn, H.T., Pickering, T.R., Musiba, C., Mabulla, A., Baquedano, E., Ashley, G., Diez-Martin, F., Santonja, M., Uribelarrea, D., Barba, R., Yravedra, J., Gidna, A., 2012b. Autochthony and artifact and fossil bone orientation patterns in Olduvai Bed I paleoanthropological assemblages: some examples from FLK North. Journal of Archaeological Science 39, 2116–2127.
Domínguez-Rodrigo, M., Diez-Martín, F., Yravedra, J., Barba, R., Bunn, H., Mabulla, A., Baquedano, E., Uribelarrea, D., Sánchez, P., Eren, M., 2014a. A study of the SHK Main Site faunal assemblage, Olduvai Gorge, Tanzania: implications for Bed II taphonomy, paleoecology, and hominin utilization of mega-fauna. Quaternary International 322-323, 153–166.
Domínguez-Rodrigo, M., Pickering, T.R., Baquedano, E., Mabulla, A., Mark, D.F., Musiba, Bunn, H.T., Uribelarrea, D., Smith, V., Diez-Martin, F., Pérez-González, A., Sánchez, P., Santonja, M., Barboni, D., Gidna, A., Ashley, G., Yravedra, J., Heaton, J.L., Arriaza, M.C., 2013b. First partial skeleton of a 1.34-million-year-old Paranthropus boisei from Bed II, Olduvai Gorge, Tanzania. PlosOne (in press).
Egeland, C.P., Domínguez-Rodrigo, M., 2008. Taphonomic perspectives on hominin site use and foraging strategies during the Bed II times at Olduvai Gorge, Tanzania. Journal of Human Evolution 55, 1031–1052.
Ferring, C.R., 1984. Intrasite spatial patterning: its role in settlement-subsistence systems analysis. In: Hietala, J. (Ed.), Intrasite Spatial Analysis in Archaeology. Cambridge University Press, Cambridge, pp. 116–126.
Gallotti, R., Piperno, M., 2004. Spatial analysis of the lithic material from level D. In: Chavaillon, J., Piperno, M. (Eds.), Studies on the Early Palaeolithic sites of Melka Kunture, Ethiopia. Istituto Italiano di Preistoria e Protostoria, Florence, pp. 599–635.
Gallotti, R., Mohib, A., El Graoui, M., Sbihi-Alaoui, F.Z., Raynal, J.-P., 2011. GIS and intra-site spatial analyses: an integrated approach for recording and analyzing the fossil deposit at Casablanca prehistoric sites (Morocco). Journal of Geographic Information System 3, 373–381.
Goldberg, P., Macphail, R.I., 2006. Practical and Theoretical Geoarchaeology. Blackwell, Malden.
Harding, P., Gibbard, P.L., Lewin, J., Macklin, M.G., Moss, E.H., 1987. The transport and abrasion of flint handaxes in a gravel-bed river. In: Sieveking, G.De.G., Newcomer, M.H. (Eds.), The Human Uses of Flint and Chert. Cambridge University Press, Cambridge, pp. 115–126.
Hay, R.L., 1976. Geology of the Olduvai Gorge. University of California Press, Berkeley.
Hosfield, R.T., 1999. The Palaeolithic of the Hampshire Basin: A Regional Model of Hominid Behaviour during the Middle Pleistocene. In: British Archaeological Reports British Series, p. 286 (Oxford).
Hosfield, R.T., Chambers, J.C., Macklin, M.G., Brewer, P., Sear, D., 2000. Interpreting secondary context "sites". A role for experimental archaeology. Lithics 21, 29–35.
Isaac, G.L., 1967. Towards the interpretation of occupation debris: some experiments and observations. Kroeber Anthropological Society Papers 37, 31–57.
Leakey, L.S.B., 1974. By the Evidence. MEmoirs, 1932–1951. Harcourt Brace Jovanovich, New York.
Leakey, M.D., 1971. Olduvai Gorge. In: Excavations in Bed I and II, vol. 3. Cambridge University Press, Cambridge, pp. 1960–1963.
Lenoble, A., 2005. Ruissellement et formation des sites préhistoriques: référentiel actualiste et exemples d'application au fossile. In: British Archaeological Reports International Series 1353 (Oxford).
Mallinsky-Buller, A., Hovers, E., Marder, O., 2011. Making time: 'Living floors', 'palimpsests' and site formation processes. A perspective from the open-air Lower Paleolithic site of Revadim Quarry, Israel. Journal of Anthropological Archaeology 30, 89–101.
Meignen, L., 1994. L'analyse de l'organisation spatiale dans les sites du Paléolithique Moyen: structures évidentes, structures latentes. Préhistoire Anthropologie Méditerranéennes 3, 7–23.
Miall, A.D., 2006. The Geology of Fluvial Deposits: Sedimentary Facies, Basin Analysis, and Petroleum Geology. Springer, Berlin.
Miall, A.D., Smith, N.D., 1989. Rivers and Their Deposits. Society of Economic Paleontologists and Mieralogists, Tulsa, Oklahoma slide set 4.
Moncel, M.H., 1993. Le site de Payre (Comune de Rompon, Ardèche). Une occupation humaine du Paléolithique moyen ancien. Quaternaire 4, 149–157.
Nanson, G.C., Croke, J.C., 1992. A genetic classification of floodplains. Geomorphology 4, 459–486.
Obregón, R.A., 2012. Estratigrafía cultural en el nivel TD10-1 de Gran Dolina, Sierra de Atapuerca (Burgos). Secuencia arqueoestratigráfica de los asentamientos contenidos en sedimento homogéneo. PhD dissertation. Universidad de Burgos, Burgos.
Petraglia, M.D., Nash, D.T., 1987. The impact of fluvial processes on experimental sites. In: Nash, D.T., Petraglia, M.D. (Eds.), Natural Formation Processes and the Archaeological Record, BAR, International Series (Oxford).
Petraglia, M., Potts, R., 1994. Water flow and the formation of Early Pleistocene artifact sites in Olduvai Gorge, Tanzania. Journal of Anthropological Archaeology 13, 228–254.
Sánchez-Yustos, P., Diez-Martín, F., Díaz Muñoz, M.I., Domínguez-Rodrigo, M., Uribelarrea, D., Fraile Márquez, C., Pérez-González, A., Mabulla, A., Baquedano, E., 2014. Percussive and knapping competences in the early Acheulean: the case of SHK main site, Olduvai Gorge, Tanzania. Quaternary International 322-323, 107–128.
Sañudo, P., Fernández-Peris, J., 2007. Análisis espacial del nivel IV de la Cova del Bolomor (La Valldigna, Valencia). Saguntum 39, 9–26.
Schick, K.D., 1986. Stone Age Sites in the Making. EXperiments in the Formation and Transformation of Archaeological Occurrences. In: BAR International Series, vol. 319 (Oxford).
Schick, K.D., 1987. Modelling the formation of Early Stone Age artifact concentrations. Journal of Human Evolution 16, 789–807.
Shackley, M.L., 1974. Stream abrasion of flint implements. Nature 248, 501–502.
Torre, de la, I., Mora, R., 2005. Unmodified lithic material at Olduvai Bed I: manuports or ecofacts? Journal of Archaeological Science 32, 273–285.
Torre, de la, I., Mora, R., 2013. The transition to the acheulean in east Africa: an assessment of paradigms and evidence from Olduvai Gorge (Tanzania). Journal of Archaelogical Method and Theory. http://dx.doi.org/10.1007/s10816-013-9176-5.
Torre, de la, I., Mora, R., Martínez-Moreno, J., 2008. The early Acheulean in Peninj (Lake Natron, Tanzania). Journal of Anthropological Archaeology 27, 244–268.
Toth, N., 1982. The Stone Technologies of Early Hominids at Koobi Fora, Kenya. AN Experimental Approach. Unpublished Ph.D. dissertation. University of California, Berkeley.
Vaquero, M., Chacón, M.G., García-Antón, M.D., Gómez de Soler, B., Martínez, K., Cuartero, F., 2012. Time and space in the formation of lithic assemblages: the example of Abric Romani level J. Quaternary International 247, 162–181.
Villa, P., 1983. Terra Amata and the Middle Pleistocene Archaeological Record of Southern France. In: University of California Publications in Anthropology, vol. 3 (Berkeley).
Williams, G.J., 2009. Rattle, a data mining GUI for R. The R Journal 1-2, 45–55.